ECOLOGICAL MODELLING 213 (2008) 209–228

available at www.sciencedirect.com

ScienceDirect

journal homepage: www.elsevier.com/locate/ecolmodel

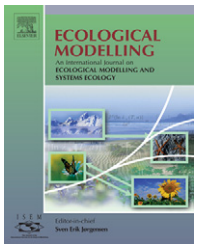

Response of tree growth to a changing climate in boreal central Canada: A comparison of empirical, process-based, and hybrid modelling approaches

Martin P. Girardin[a,b,*], *Frédéric Raulier*[b], *Pierre Y. Bernier*[a], *Jacques C. Tardif*[c]

[a] *Natural Resources Canada, Canadian Forest Service, Laurentian Forestry Centre, 1055 du P.E.P.S., P.O. Box 10380, Stn. Sainte-Foy, Quebec, QC G1V 4C7, Canada*

[b] *Faculté de foresterie et de géomatique, Université Laval, Quebec, QC G1K 7P4, Canada*

[c] *Centre for Forest Interdisciplinary Research (C-FIR), University of Winnipeg, 515 Portage Avenue, Winnipeg, MB R3B 2E9, Canada*

ARTICLE INFO

Article history:
Received 6 June 2007
Received in revised form
2 December 2007
Accepted 11 December 2007
Published on line 7 February 2008

Keywords:
Climate change
Dendroclimatology
Empirical modelling
Process-based modelling
Hybrid modelling
Tree-ring growth increments
Forest net primary productivity
Boreal plains of Canada

ABSTRACT

The impact of $2 \times CO_2$ driven climate change on radial growth of boreal tree species *Pinus banksiana* Lamb., *Populus tremuloides* Michx. and *Picea mariana* (Mill.) BSP growing in the Duck Mountain Provincial Forest of Manitoba (DMPF), Canada, is simulated using empirical and process-based model approaches. First, empirical relationships between growth and climate are developed. Stepwise multiple-regression models are conducted between tree-ring growth increments (TRGI) and monthly drought, precipitation and temperature series. Predictive skills are tested using a calibration–verification scheme. The established relationships are then transferred to climates driven by $1\times$ and $2 \times CO_2$ scenarios using outputs from the Canadian second-generation coupled global climate model. Second, empirical results are contrasted with process-based projections of net primary productivity allocated to stem development (NPP_s). At the finest scale, a leaf-level model of photosynthesis is used to simulate canopy properties per species and their interaction with the variability in radiation, temperature and vapour pressure deficit. Then, a top-down plot-level model of forest productivity is used to simulate landscape-level productivity by capturing the between-stand variability in forest cover. Results show that the predicted TRGI from the empirical models account for up to 56.3% of the variance in the observed TRGI over the period 1912–1999. Under a $2 \times CO_2$ scenario, the predicted impact of climate change is a radial growth decline for all three species under study. However, projections obtained from the process-based model suggest that an increasing growing season length in a changing climate could counteract and potentially overwhelm the negative influence of increased drought stress. The divergence between TRGI and NPP_s simulations likely resulted, among others, from assumptions about soil water holding capacity and from calibration of variables affecting gross primary productivity. An attempt was therefore made to bridge the gap between the two modelling approaches by using physiological variables as TRGI predictors. Results obtained in this manner are similar to those obtained using climate variables, and suggest that the positive effect of increasing growing season length would be counteracted by increasing summer temperatures. Notwithstanding uncertainties in these simulations (CO_2 fertilization effect,

* *Corresponding author at*: Natural Resources Canada, Canadian Forest Service, Laurentian Forestry Centre, 1055 du P.E.P.S., P.O. Box 10380, Stn. Sainte-Foy, Quebec, QC G1V 4C7, Canada. Tel.: +1 418 648 5826; fax: +1 418 648 5849.
E-mail address: Martin.Girardin@rncan.gc.ca (M.P. Girardin).

doi:10.1016/j.ecolmodel.2007.12.010

feedback from disturbance regimes, phenology of species, and uncertainties in future CO_2 emissions), a decrease in forest productivity with climate change should be considered as a plausible scenario in sustainable forest management planning of the DMPF.

1. Introduction

Terrestrial vegetation responds to weather and climate through a variety of physiological, demographic, and ecosystem functions (Bonan, 2002). Together, these functions determine where plant species grow, how well they grow, and how their arrangement within the communities changes over time (Bonan, 2002). In this context, any changes in the state of weather and climate will affect terrestrial vegetation. The impact may be direct via interference with the plants' physiology (e.g. growth, bud formation, flowering) or indirect via changes in the stand dynamics (e.g. regime of disturbances) (Loehle and LeBlanc, 1996; Weber and Flannigan, 1997).

Increases in atmospheric CO_2 concentrations are expected to cause significant changes in the climate of northeastern Manitoba, Canada (Boer et al., 2000a,b). Simulations for years 2040–2049 show a summer warming of 4–5 °C and a winter warming of 5–8 °C as a consequence of this forcing (Laprise et al., 2003). In southwestern Manitoba, the warming is expected to be less severe, with a trend toward a decrease in precipitation by approximately 10–20% (Laprise et al., 2003). These changes in climate are expected to cause an increasing drought stress on vegetation occupying the lower range limits of Manitoba forests (Hogg, 1994; Hogg and Bernier, 2005). Lakes, wetlands and peatlands would be profoundly affected, and forest productivity could be greatly reduced, especially following periods of drought-induced mortality (Hogg and Bernier, 2005). This concern is especially present after record dry spells during 2001–2003 led to a widespread *Populus tremuloides* Michx. forest mortality over southwestern Canada (Hogg et al., 2005). Additionally, Flannigan et al. (2005) predicted large increases in area burned by wildfire throughout Canadian boreal forests. Wildfire responds rapidly to changes in weather and climate in comparison to vegetation; hence, the rate and magnitude of fire regime-induced changes to Manitoba forest landscapes could greatly exceed anything expected owing to climate change alone (Weber and Flannigan, 1997). Despite the uncertainties associated with climate models, the development of adaptation management strategies in the forest sector is a necessity (Spittlehouse and Stewart, 2003).

Our ability to predict the impact of greenhouse gas driven climate change on tree growth at the lower range limits of Manitoba forests is limited unless we understand the physiological processes governing forest productivity. At the lower margin of boreal forests, the statistical relationship between tree radial growth and climate can be summarized by a combination of two driving climate components. The first relates to seasonal drought whereas the other relates to the length of the growing season (Graumlich, 1993; Tardif and Bergeron, 1997; Hofgaard et al., 1999; Girardin and Tardif, 2005; Girardin et al., 2006). The drought component defines the process by which soil moisture is sufficient to maintain foliage water potential, minimize vapour pressure deficits, and allow for optimal tree growth and assimilation of carbohydrates (Dang et al., 1998; Bonan, 2002). The second component relates to the onset and duration of the growing season. Warm winter and spring temperatures are presumed to interfere with budbreak phenology (Myking and Heide, 1995; Linkosalo, 2000; Chuine, 2000; Chuine and Beaubien, 2001; Bonan, 2002). Bud growth does not respond to temperatures before a minimum amount of chilling units (weeks or months) or until the accumulation of certain heat sums above a specific base temperature. Early bud growth releases can notably expose trees to risk of frost damage and, the next summer, to a decrease in total foliage area, in assimilated carbohydrates, and in growth. Conifers can take advantage of earlier springs due to evergreen foliage (Graumlich, 1993; Tardif and Bergeron, 1997; Girardin and Tardif, 2005) and if weather is favourable they can photosynthesize throughout late autumn, winter and early spring (Bonan, 2002).

The direct impact of climate change on tree growth at the lower range limit of Manitoba forests will depend on the response of tree species to changes in the drought regime and growing season length (Loehle and LeBlanc, 1996; Hogg and Bernier, 2005). Due to the difficulty in determining how climate change will affect these two components of tree growth, prediction under a future climate remains challenging. The first objective of this study is to determine the extent to which the introduction of ecophysiological concepts can improve the capacity of dendroclimatological models to explain year-to-year variability in tree-ring growth increments (TRGI) in boreal tree species *Pinus banksiana* Lamb., *P. tremuloides* Michx. and *Picea mariana* (Mill.) BSP growing in the Duck Mountain Provincial Forest (DMPF). The second objective is to use the resulting hybrid models to estimate future TRGI in a case study of climate change, and look at how these projections depart from those obtained from empirical and process-based modelling approaches.

2. Materials and methods

2.1. Study area

The DMPF (51°40′N, 100°55′W) is part of the Boreal Plains ecozone, a transition zone between the boreal forest to the north and the aspen parkland and prairie to the south (Fig. 1). The DMPF is approximately 376,000 ha in size and ranges in altitude from 300 to 400 m above mean sea level at the eastern escarpment to 825 m at Baldy Mountain. The DMPF lies within a mid-boreal climate with predominantly short, cool summers and cold winters. For the period 1971–2000, at Swan River (52°30′N, 101°13′, elevation 346.6 m above sea level), mean monthly temperatures ranged from −18.2 °C in January to 18.1 °C in July. Average total annual precipitation was 530.3 mm with most precipitation falling as rainfall between May and September (Ecological Stratification Working Group,

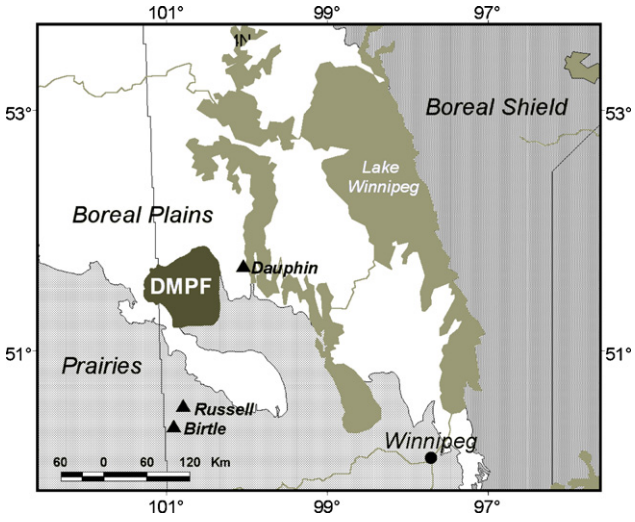

Fig. 1 – Map showing the geographical location of Duck Mountain Provincial Forest (DMPF) in Manitoba, Canada. Meteorological stations are indicated by filled triangles.

1996; Environment Canada, 2000). Compared with the surrounding lowlands, however, the DMPF plateau has cooler summers and winters and could also receive about 50% more precipitation (Manitoba Provincial Parks Branch, 1973).

The DMPF is composed predominantly of deciduous forest especially in the lowlands, with coniferous boreal forest in the upland areas and mixedwood deciduous/coniferous forest in the midlands (Ecological Stratification Working Group, 1996; Kenkel and Hamel, 2000; Tardif, 2004; Sutton and Tardif, 2007). Medium to tall closed stands of *Betula papyrifera* Marsh., *P. tremuloides* and *Populus balsamifera* L. with *P. mariana* and *Picea glauca* (Moench) Voss, and *Abies balsamea* (L.) Mill. occurring in late successional stages, are the most abundant. Stands of *P. banksiana* occur on dry, sandy sites. Deciduous stands have a diverse understory of shrubs and herbs; coniferous stands tend to promote feathermoss. Cold and poorly drained fens and bogs are covered with *Larix laricina* (Du Roi) K. Koch and *P. mariana* (Ecological Stratification Working Group, 1996).

2.2. Tree-ring growth increment data

Tree-ring width data sets of *P. banksiana*, *P. tremuloides*, and *P. mariana* (one data set for upland sites and one for lowland sites), previously published by Girardin and Tardif (2005), were used for this study for calibration of the empirical models (Appendix A). The tree-ring samples originated from a sampling of a systematic grid of UTM squares (10 km × 10 km) overlaid on the DMPF (Tardif, 2004). Site (forest polygon) selection was constrained by accessibility and a total of 263 sites were located and geo-referenced. At each site, 8–10 trees were sampled. Fire-scarred trees, snags and downed woody debris (charred or not) were also collected to extend the chronologies further back in time. Tree-ring samples were treated using standard procedures. Measurement series were crossdated, detrended using a cubic smoothing spline giving a 50% frequency response of 60 years (Cook and Peters, 1981), and biological persistence (autocorrelation) was removed using autoregressive modelling (Cook and Holmes, 1986). Biweight robust means of the residual series were computed for each data set to create the TRGI (unitless index values). The four TRGI were constructed using the tree-ring chronology processing program ARSTAN (Holmes, 1999).

2.3. Climate data

Monthly means of daily maximum and minimum temperatures (from the Birtle [1905–1998] and Dauphin [1904–1999] meteorological stations; Fig. 1) and total monthly precipitation data (from the Birtle [1918–1999], Dauphin [1912–1999], and Russell [1916–1990] meteorological stations) from Vincent and Gullett (1999) and Mekis and Hogg (1999), respectively, were used as growth predictor variables. Additionally, monthly regional averages of the daily Drought Code (1912–1999) (Girardin et al., 2004) were used. The Drought Code was computed from daily data of 12 meteorological stations. The Drought Code was developed to represent the net effect of daily changes in evapotranspiration and precipitation on cumulative moisture depletion in soils. It reflects the moisture content of organic matter averaging about 18 cm in thickness and 25 kg m^{-2} in dry mass, for a bulk density of 138.9 kg m^{-3}. Because soil moisture losses over time usually follow a negative exponential, the Drought Code was found to represent quite well certain types of slow-drying organic matter (time constant about 52 days). The equation linking the Drought Code (DC) to its moisture equivalent (Q) from Van Wagner (1987) is

$$Q = 800\, e^{(-DC/400)} \quad (1)$$

The 400 constant in Eq. (1) represents the maximum theoretical moisture content of the organic layer represented by the Drought Code, which roughly corresponds to the water-holding capacity of the soil (100 mm) (Van Wagner, 1987). There are no absolute guidelines as to the meaning of the Drought Code values but generally speaking, values below 200 are considered low and 300 may be moderately dry in most parts of the country. A rating above 300 indicates severe drought.

Regional climate data files were created by averaging data (i.e. temperature, precipitation and Drought Code) from all stations following the procedure described in Holmes (1999) (homogeneity testing, station adjustments for mean and standard deviation, and station averaging).

2.4. Climate change scenario

Prediction of future tree growth was made using simulated daily temperature (minimum and maximum) and precipitation data collected from the Canadian second-generation coupled global climate model (CGCM2) over time horizons 1961–1989 and 2041–2060 (Flato et al., 2000; Flato and Boer, 2001; http://www.cccma.bc.ec.gc.ca). Global climate models are time-dependent numerical representations of the atmosphere and its phenomena over the entire Earth, using the equations of motion and including radiation, photochemistry, and the transfer of heat, water vapour, and momentum. Future climate scenarios are built based on the effects of various concentrations of greenhouse gases and other pollutants

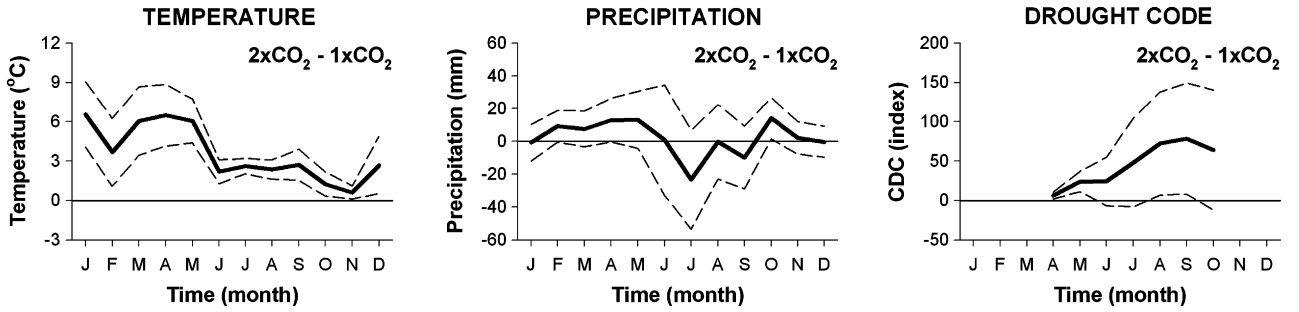

Fig. 2 – Average monthly mean temperature, total precipitation and mean Drought Code differences between 2× and 1 × CO_2 driven climate scenarios (thick lines). The period is January 'J' to December 'D'. Dashed lines: 95% confidence interval: when the zero line crosses the confidence interval, the null hypothesis of 'no significant difference between scenarios' cannot be rejected at the 95% level.

within the atmosphere on the Earth-atmosphere system. The current case study uses the GHG+A IPCC B2 scenario run (Nakicenovic et al., 2000), which includes both greenhouse gas and sulphate aerosol forcing, with a rise in CO_2 from 330 parts per million by volume (ppmv) in year 1850 to 659 ppmv in year 2040 and 740 ppmv in year 2070. The 1961–1989 and 2041–2060 time horizons hence correspond to equivalent carbon dioxide concentrations $1 \times CO_2$ and $2 \times CO_2$, respectively. The CGCM2 point grid corresponding to 101.25W, 50.10N was selected for this study. Differences in means between meteorological station data and simulated monthly climate data over 1961–1989 were tested (p(t-test) < 0.05)) and, when necessary, adjustments were applied to simulated data; variance between observed and simulated data was not significantly different (for most variables p(F-test) > 0.05) and thus was not adjusted. Overall, the simulation outputs included significant increases of monthly mean temperatures (by up to 6 °C in the spring season) and of monthly mean drought severity (significant in spring and late summer) (Fig. 2). Trends like these are also typical of CGCM3 (Flato et al., 2000) and ECHAM4 (Roeckner et al., 1996) simulations, although the trends in temperature and drought severity are stronger (weaker) in scenarios of greater (lower) total global CO_2 emissions (Girardin and Mudelsee, in press). While we restrict our analyses to this CGCM2 case study, it should be kept in mind that there may be some variability around the projected tree growth trends, depending on models and scenarios of CO_2 emissions.

2.5. *Empirical models of tree-ring growth increments*

The empirical models of TRGI were developed as follows. For each of the four TRGI, a least-squares stepwise multiple regression employing a backward selection was used to calibrate the TRGI against the monthly temperature (maximum and minimum), precipitation, and Drought Code data (period 1912–1999):

$$y_j = \sigma + \beta_1 x_{1j} + \beta_2 x_{2j} + \cdots + \beta_m x m_{mj} + \varepsilon_j \quad (2)$$

where y_j is the annual value of TRGI, x_j the climate data, β the regression coefficients, and ε_j is the error (Foster and LeBlanc, 1993; Laroque and Smith, 2003). The period of analysis included July of the year previous to ring formation to October of the year of ring formation. Hence, a total of 59 potential predictor variables were included in the stepwise models. Minimum tolerance for entry into the models was set at 0.1 (prevents the entry of a variable that is highly correlated with the independent variables already included in the model). Alpha-to-enter and alpha-to-remove were set at 0.10 and 0.05, respectively.

Next, the stability of each regression model was tested using a split sample calibration–verification scheme (e.g., Cook et al., 1994; Cook and Kairiukstis, 1990). The procedure consisted in calibrating the models over the period 1912–1969. Once estimated for the calibration period, the regression coefficients were applied to the monthly climate variables over the verification period 1970–1999 to produce a series of TRGI estimates. The strength of the relationship between TRGI estimates and observations was measured using the Pearson r^2, the reduction of error (RE) and the product means test (PM) (Cook et al., 1994). The RE statistic is a measure of the explained variance in the verification period. If the prediction does better than the average of the dependent period, then it has a positive value between zero and one. This statistic is highly sensitive to the presence of trends in the data or to a few bad estimates. The PM test calculates the products of the deviations and collects the positive and negative products in two separate groups based on their signs. The values of the products in each group are summed, and the means computed. The difference between the absolute values of the two means can be tested for significance using the t statistics. A significant PM test result indicates that the magnitude and the direction of these changes are statistically significant. Stepwise multiple regressions were conducted using the software Systat 11 (Systat Software Inc., 2004). The program VFY (Holmes, 1999) was used for calculation of the RE and PM verification statistics.

2.6. *Process-based modelling approach of net primary productivity*

Process-based models serve as direct links between the climate and the production of wood fibre (Hunt et al., 1991; Landsberg, 2003a,b; Rathgeber et al., 2003; Misson et al., 2004). The process-based productivity model StandLEAP version 0v6 (Raulier et al., 2000; Hall et al., 2006) was used to produce

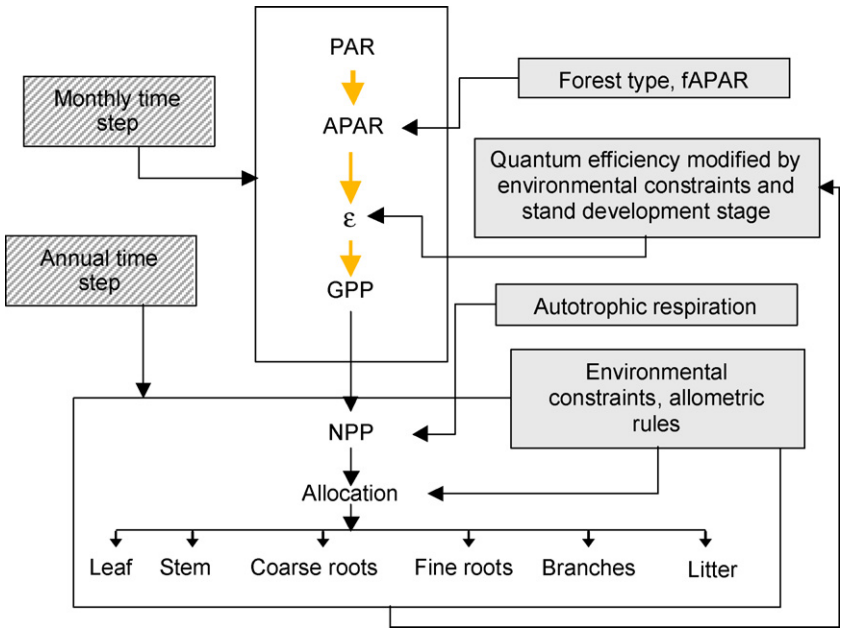

Fig. 3 – StandLEAP schematic description. PAR: photosynthetically active radiation; APAR: absorbed PAR by the canopy; fAPAR: fraction of PAR absorbed by the canopy; ε: radiation use efficiency; GPP: gross primary production; NPP: net primary production.

estimates of net primary productivity (NPP) and net primary productivity allocated to stem development (NPP_s). StandLEAP is based on the 3PG model (Landsberg and Waring, 1997; Landsberg, 2003a), and is a generalized stand model (i.e., it is not site specific but needs to be parameterized for individual species) applicable to even-aged, relatively homogeneous forests. Application of StandLEAP to any particular stand does not involve the use of error reduction techniques.

In StandLEAP (see Fig. 3), absorbed photosynthetically active radiation (APAR) is related to gross primary productivity (GPP, mol m^{-2} $month^{-1}$) using a radiation use efficiency coefficient (RUE):

$$GPP = APAR \times RUE \quad (3)$$

where

$$RUE = \overline{RUE} \times f_1 f_2 \ldots f_n \quad (4)$$

$\overline{RUE}$ represents a species-specific mean value of RUE. The value of RUE differs among species and through time because of the occurrence of environmental constraints on the capacity of trees to use APAR to fix carbon. Each constraint takes on the form of a species-specific multiplier ($f_1, \ldots, f_n$) with a value usually close to unity under average conditions, but which can decrease towards zero to represent increasing limitations (e.g., soil water deficit), or increase above 1.0 as conditions improve towards optimum (e.g., temperature):

$$f_n = 1 + \beta_{lx}\left(\frac{x - \bar{x}}{\bar{x}}\right) + \beta_{qx}\left(\frac{x - \bar{x}}{\bar{x}}\right)^2 \quad (5)$$

Parameters β_{lx} and β_{qx} represent the linear and quadratic effects of the f_n variable on RUE and $\bar{x}$ is the mean value of the variable over the period of calibration. The multipliers ($f_1, \ldots, f_n$) account for non-linearity in time and space that cannot be accounted for by a constant value of RUE. Multipliers are used to represent the effect of soil water content (f_θ as in Landsberg and Waring, 1997; Bernier et al., 2002), frost (f_F as in Aber et al., 1995) (both limited to a maximum of 1.0), mean maximum and minimum daily air temperature, vapour pressure deficit (VPD), monthly radiation, and leaf area index (where values greater than 1.0 are possible) on GPP (Appendix A).

Bud burst and growth resumption in spring occur after the accumulation of a certain heat sum above a specific base temperature (Appendices) (Hänninen, 1990). Monthly APAR is adjusted throughout the growing season for changes in leaf area due to phenological development, as in the PnET model (Aber and Federer, 1992). Mean foliage retention time (number of growing seasons) varies from one season for *P. tremuloides* to ten seasons for *P. banksiana* (Appendices). Leaf fall is set to start after Julian day 270 when the lower base temperature for growing degree-days sum is reached (Aber and Federer, 1992).

Respiration is computed as a fixed proportion of GPP (Waring et al., 1998; Malhi et al., 1999), and net primary productivity (NPP; g m^{-2} $month^{-1}$) is computed monthly as GPP minus respiration. As in 3-PG, part of NPP is first allocated to fine roots (Landsberg and Waring, 1997, Eq. (13)) on a yearly basis and then to replacement of carbon biomass due to leaf and fine woody litter turnover. The remaining NPP is then allocated to stand carbon compartments (Fig. 3) foliage, branches, coarse roots, and stems (hereafter called NPP_s) (Hall et al., 2006).

In StandLEAP, most of the basic climate influences on productivity are encapsulated within the RUE term and its parameters in Eq. (5), and these influences stem from the leaf-level interaction between photosynthesis and climatic variables. Parameter values in Eq. (5) for all environmental

variables except soil water content and frost are therefore derived from prior finer-scale simulation results. For each species, prior simulations of canopy-level GPP and transpiration were carried out using FineLEAP, a species-specific multi-layer canopy gas exchange model (Raulier et al., 2000; Bernier et al., 2001, 2002). In FineLEAP, the representation of photosynthesis is based on the equations of Farquhar et al. (1980) parameterized for each species from leaf-level instantaneous gas exchange measurements. Transpiration is computed using the energy balance approach of Leuning (1995). Canopy photosynthesis A_c (mol $(m^2$ ground$)^{-1}$ s^{-1}) is estimated as:

$$A_c = L^* \sum_{i=1}^{n} \nu_i \sum_{\theta_l} \sum_{\alpha_l} [\nu_{\theta,\alpha}(\nu_b A_n(\bar{I}_{l.b0} + \bar{I}_{l.d}) + (1 - \nu_b) A_n(\bar{I}_{l.d}))] \quad (6)$$

where L^* is the leaf area index of the canopy, ν_i is the distribution frequency of leaf area within a class i of leaf mass per unit area (LMA), $\nu_{\theta,\alpha}$ is the distribution frequency of leaf area within a given class of leaf angle, ν_b corresponds to the fraction of sunlit leaf area in a given LMA layer, $A_n(\bar{I}_s)$ is net leaf photosynthesis for a mean intercepted irradiance $\bar{I}_s$, $\bar{I}_{l.b0}$ is the direct (beam) radiation reaching the LMA layer l, and $\bar{I}_{l.d}$ is the diffuse radiation reaching the LMA layer l. Sixty leaf angular classes are considered (five for the zenith and 12 for the azimuth). The time step is hourly. The model simulates canopies aspatially as layers of foliage of equal properties by using the frequency distribution of the leaf area by classes of specific leaf mass, and of shoot age in the case of evergreen species. This aspatial approach rests on the strong relationship between specific leaf mass, shoot age (for conifers), and both the photosynthetic properties of the foliage and the average light climate impinging upon it (Bernier et al., 2001).

The capacity of FineLEAP to simulate canopy-level gas exchanges has been verified by comparing hourly (Bernier et al., 2001) and daily (Raulier et al., 2002) measurements of plot-level transpiration to simulated values for two different stands of sugar maple (*Acer saccharum* Marsh.). The comparison revealed an absence of bias in the simulations and a fit to measured transpiration with values of R^2 of 0.72 (hourly measurements, Bernier et al., 2001) and of 0.94 (daily measurements, Raulier et al., 2002).

The procedure for estimating the value of FineLEAP parameters has been described in detail in Raulier et al. (2000) and Bernier et al. (2001). In brief, a complete set of gas exchange measurements is required, including the sensitivity of shoot photosynthesis to PAR, temperature and VPD, and the characterization of the shoot physiological and light-capturing properties with shoot age and surrounding average light environment. Ecophysiological and canopy structure data for *P. banksiana*, *P. mariana* and *P. tremuloides* were drawn mostly from the BOREAS (Sellers et al., 1997) datasets that have been archived at the ORNL-DAAC (Newcomer et al., 2000). These data were originally obtained on mature trees growing in the boreal forest near Thompson (Province of Manitoba, Canada; BOREAS study TE-09, laboratory data, Dang et al., 1997, 1998). The light-capturing properties were derived from BOREAS studies TE-06 (Gower et al., 1997), TE-23 (Fournier et al., 1997) and RSS-07 (Chen, 1996). The contribution of the various researchers who have made their data available through this collective effort is sincerely acknowledged. Values of shoot boundary layer conductance to heat for *P. banksiana* and *P. mariana* were derived from Smith (1980) and Landsberg and Ludlow (1970), respectively. The leaf boundary layer conductance for *P. tremuloides* was derived as described by Leuning (1995, therein Eq. (1)) and required the average leaf width, derived from Middleton et al. (1997, their Table 3).

For the three species of interest, hourly values of transpiration and of GPP were simulated in FineLEAP using climate sequences of hourly values of temperature and radiation obtained from BOREAS (northern and southern study areas old jack pine stands (98°37′19″W, 55°55′41″N and 104°41′20″W, 53°54′58″N, respectively) from 1994 to 1996). FineLEAP simulations were repeated for each climate sequence, by species and for a range of leaf area indices (2–8 m^2/m^2). Hourly values of transpiration, of GPP, and of environmental variables derived from or used in FineLEAP simulations were rolled up into a monthly dataset. This new synthetic dataset was then used to fit simultaneously Eqs. (3) and (4), in which modifier variables were expressed as in Eq. (5). All parameters were estimated simultaneously using the MODEL procedure of the SAS Software (SAS Corporation, Cary, North Carolina, USA). Variables for which modifiers were initially computed for GPP (Eq. (2)) and transpiration (Eq. (5)) were monthly average temperature and VPD, monthly PAR and leaf area index. The fit was performed in an iterative procedure with the gradual inclusion of modifier variables in a declining order of significance. Only variables that reduced the residual mean square error by more than 5% were retained (Raulier et al., 2000). When the quadratic term of the modifier equation (Eq. (3)) was significant, its linear term was always kept even when non-significant (Draper and Smith, 1998).

Necessary stand and climate data inputs to StandLEAP included soil textures, soil depths (a parameter to be determined), species cover, tree density and biomass, monthly mean daily maximum and minimum temperature, and monthly total precipitation. Climate data were those used in the empirical modelling approach. Precipitation interception by the canopy was fixed at 23% (Van Wagner, 1987; Bonan, 2002; Morris et al., 2003). Soil texture and forest stand properties were derived from DMPF temporary sample plots (TSP) classified as what we assumed to be "pure" stands (i.e., where more than 75% of plot basal area was contributed by the dominant species) and for dominant soil types. TSP data were gathered from the Forest Lands Inventory initiated by Louisiana Pacific Canada Ltd. – Forest Resources Division and Manitoba Conservation – Forestry Branch. For each TSP, aboveground biomass was estimated using national biomass equations (Lambert et al., 2005). Lambert et al. (2005) used biomass data previously collected in the boreal forest regions of the Prairie Provinces, Northwest Territories and Yukon to develop allometric functions relating either tree height (m) and diameter at breast height (DBH), or simply DBH, to the different components of aboveground tree biomass (kg $tree^{-1}$) by species. These functions were then applied to all trees in each TSP, and the individual tree biomass values summed to estimate stand-level biomass density (Mg ha^{-1}). We applied these stand-level functions of biomass to the stand attributes in the TSP database to assign a biomass estimate. TSP data were averaged by

Table 1 – Average properties of the temporary sample plots of the DMPF Lands Inventory used as the basis for the StandLEAP simulations

Forest types	Elevation[a] (m)	Slope (°)	Aspect (°)	N_{ha}[b] (n/ha)	W_{abg}[c] (Mg/ha)	Soil type	*n* plots
Pinus banksiana (Conifer)	705.2 (6.5)	3.52 (2.20)	235 (71)	850 (554)	161.9 (70.5)	Silty clay	6
Picea mariana uplands (Conifer)	700.5 (35.2)	4.87 (4.39)	169 (107)	788 (568)	81.6 (65.0)	Clay loam	24
P. mariana lowlands (Conifer)	676.0 (58.4)	1.44 (2.12)	115 (130)	747 (752)	86.6 (63.1)	Silty clay	38
Populus tremuloides (Hardwood)	604.2 (62.6)	2.55 (3.32)	144 (129)	505 (309)	117.1 (89.7)	Silty clay	64

Standard deviations appear in parentheses.

[a] Above sea level.

[b] Number of stems per hectare.

[c] Aboveground biomass.

species and soil type prior to being entered into StandLEAP (Table 1).

The soil depth parameter (for which there are no field data available) was determined by means of tuning and maximizing the correlation between the simulated NPP_s and TRGI (Misson, 2004). The sensitivity to soil depth is inherent to the inclusion of soil water as a modifier of transpiration (Bernier et al., 2002; Bonan, 2002). Variations in soil depth exert a sig-

Table 2 – Calibration and verification statistics of empirical models of tree-ring growth increments (TRGI)

	P. banksiana	*P. mariana* uplands	*P. mariana* lowlands	*P. tremuloides*
Calibration 1912–1999				
Number of predictor variables selected by the stepwise model	6	9	9	13
R^2	0.514	0.523	0.482	0.563
Adjusted r^2	0.478	0.468	0.422	0.486
Standard error of the estimate	0.097	0.098	0.087	0.129
Calibration 1912–1969				
R^2	0.504	0.562	0.492	0.611
Adjusted r^2	0.446	0.478	0.397	0.496
Standard error of the estimate	0.099	0.095	0.081	0.142
Verification 1970–1999				
Correlation (r^2)[a]	0.465[a]	0.428[a]	0.445[a]	0.283[a]
Reduction of error (RE)[b]	0.465[b]	0.413[b]	0.366[b]	−0.047
Product mean test (PM)[c]	2.538[c]	3.626[c]	3.166[c]	1.718[c]
Monthly predictors				
Temperature (minimum and maximum)	$-T_{max}$ August$_{-1}$ $-T_{max}$ February	$-T_{min}$ August$_{-1}$ $+T_{min}$ August $+T_{min}$ October $+T_{max}$ January $-T_{max}$ February	$-T_{min}$ October$_{-1}$ $+T_{min}$ August $-T_{max}$ August$_{-1}$ $+T_{max}$ January $-T_{max}$ February $-T_{max}$ August	$-T_{min}$ September$_{-1}$ $+T_{min}$ December$_{-1}$ $-T_{min}$ February $-T_{min}$ March
Precipitation	 +*P* August	+*P* December$_{-1}$		+*P* August$_{-1}$ +*P* December$_{-1}$ −*D* July$_{-1}$
Drought code	−*D* July +*D* September −*D* October	−*D* July +*D* September −*D* October	−*D* July +*D* September −*D* October	+*D* September$_{-1}$ −*D* October$_{-1}$ +*D* May −*D* July +*D* September −*D* October

Monthly climate variables selected as TRGI predictors are also shown: *T* is the temperature, *P* is the precipitation and *D* is the Drought Code; + and − indicate the sign of coefficients; months previous to the year of ring formation (July–December) are labelled with "−1".

[a] Significant at $p < 0.05$ if r^2 (*r* square) > 0.10.

[b] Considered satisfactory if RE > 0. Whenever RE is greater than zero, the prediction is considered as being a better estimate of growth than the calibration period mean.

[c] Considered significant at $p < 0.05$ if PM > 1.70. A significant PM test result indicates that the magnitude and the direction of year-to-year changes are statistically significant.

nificant effect on NPP_s (Woodward and Osborne, 2000) because water storage capacity of the soil determines how much water is available for transpiration during dry periods, thereby affecting NPP_s (Kleidon and Heimann, 1998; Bernier et al., 2002, 2006). If the depth chosen for the simulation is shallower than the actual extension of the roots, NPP_s will appear overly responsive to low soil water content. If the depth chosen is deeper than the actual rooting depth, NPP_s will appear resistant to a drop in soil water content (Woodward and Osborne, 2000; Bernier et al., 2002). In this study, NPP_s was simulated over the interval 1912–1999 for depths ranging from 200 mm to 4000 mm and the values that gave the best Spearman rank correlations (Zar, 1999) with the TRGI were retained for forecasting.

2.7. *Hybrid model of tree-ring growth increments*

The empirical modelling provides evidence of statistical association between growth and climate, but only hints at possible biological mechanisms (Arbaugh and Peterson, 1989; Foster and LeBlanc, 1993). The approach includes over 50 potential predictor variables, some of which can be retained in spite of weak biological justification or because of spurious relationships (Arbaugh and Peterson, 1989). This problem can be partly addressed by including variables descriptive of soil water content, such as the Drought Code, seasonal variables such as growing degree days, and other modifiers that reflect climatically induced reductions in growth (Foster and LeBlanc, 1993). These predictors may be more useful than precipitation or temperature alone in explaining differences in the performance of trees in different situations (Landsberg, 2003b; Rathgeber et al., 2005). Conversely, the process-based model attempts to predict the products by describing the processes that lead to them through the simulation of responses to external driving variables and interactions between processes (Landsberg, 2003b). Although limited in many respects, the process-based model offers significant advantages over the TRGI empirical models for understanding and predicting forest behaviour (Landsberg, 2003a,b).

In an effort to capture the strengths of both approaches, a certain number of hybrid TRGI models have been developed recently in a quest to improve sensitivity to environmental variability (Foster and LeBlanc, 1993; Woollons et al., 1997; Baldwin et al., 2001; Snowdon, 2001). Generally, these hybrid models incorporate a limited number of climatic and edaphic variables directly into the empirical models. In the present project, we combined results from the StandLEAP process-based model with the empirical TRGI model in a fashion similar to that employed by Foster and LeBlanc (1993). We used a least-squares stepwise multiple regression employing a backward selection (Eq. (2)) to calibrate TRGI of all three species against physiological variables obtained from StandLEAP (under the optimized soil depths).

2.8. *Simulations for climate change scenario*

After development of the empirical models of TRGI (Eq. (2)) and verification of their predictive skills, the regression coefficients estimated for the 1912–1999 calibration period were applied to the CGCM2 data (temperature, precipitation and Drought Code) and prediction of future TRGI was made. For NPP_s modelling, observed climate data were simply substituted by the CGCM2 data. Changes in average growth and NPP_s from the $1 \times CO_2$ to the $2 \times CO_2$ scenarios were subsequently tested using a *t*-test statistic (Zar, 1999). This parametric procedure tests the null hypothesis "constant average growth" against two-sided alternatives such as "increasing or decreasing average growth". One seeks to disprove the null hypothesis of a constant average growth from one time slice to the next when the *p* value is lower than 0.05. In cases where changes in NPP_s were detected between periods, month-by-month NPP comparisons were carried out between periods in order to detect the time of the year during which a change in NPP was most significant.

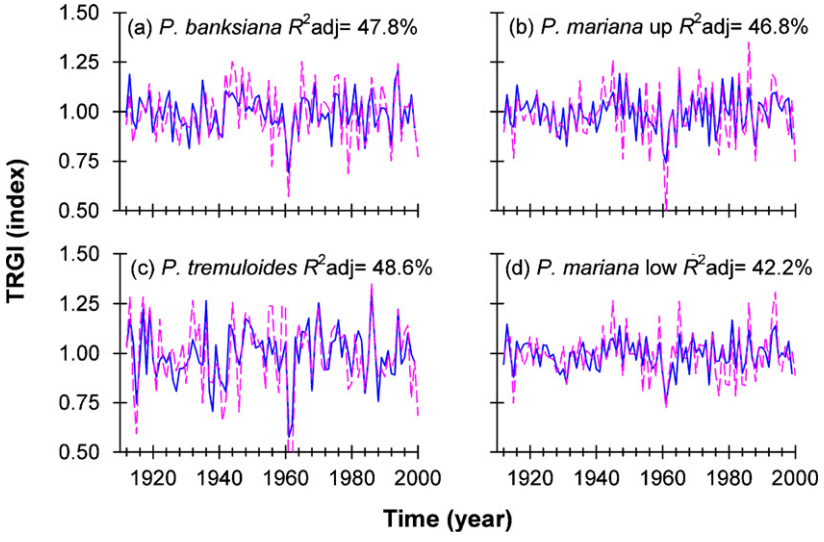

Fig. 4 – Observed (dashed lines) and estimated tree-ring growth increments (TRGI; solid lines). The adjusted R^2 shows the amount of variance accounted for by the estimates over the 1912–1999 calibration period. Species are *Pinus banksiana*, *Populus tremuloides*, and *Picea mariana* from uplands and lowlands.

3. Results

3.1. Evaluation of TRGI empirical model performance

Empirical models of TRGI for the DMPF were developed for all species under study. The amount of variance in observed TRGI explained by the climate variables ranged from 48.2% to 56.3% (Table 2; Fig. 4), with the highest R^2 obtained for *P. tremuloides*. Monthly climate variables selected as potential TRGI predictors (Table 2) are 'qualitatively' similar to those obtained from bootstrap response functions (Girardin and Tardif, 2005) and redundancy analyses (Girardin et al., 2006).

The fidelity of the empirical models of TRGI was evaluated with the r^2, RE and PM verification statistics using a split sample calibration–verification scheme (Table 2). High RE ($RE > 0.30$) and correlation ($r^2 > 0.36$) indicated tendencies for the *P. banksiana* and *P. mariana* empirical models to adequately reproduce high and relatively low frequency variations in TRGI (Fig. 4). The PM test indicated significant predictive skills to reproduce the magnitude and direction of year-to-year changes. The *P. tremuloides* empirical model showed little predictive skills in spite of the high sensitivity of its growth to climate (Table 2). Potential causes for low model predictive skills are discussed further in the text.

Table 3 – Ratios of average TRGI for $2 \times CO_2/1 \times CO_2$ scenarios

Ratio	$2 \times CO_2/1 \times CO_2$
P. banksiana	0.95**
P. mariana uplands	0.98
P. mariana lowlands	0.97*
P. tremuloides	0.95**

The differences in mean were tested for significance using the *t*-test statistic. This parametric procedure tests the null hypothesis "constant average growth" against two-sided alternatives such as "increasing (ratio > 1.00) or decreasing (ratio < 1.00) average growth". Differences tested significant at the 95% level are marked with one asterisk (*); differences significant at the 99% level are marked with two asterisks (**).

3.2. Forecasts of future TRGI

Prediction of TRGI in climate change scenarios was conducted by applying the regression equations estimated from the calibration of the period 1912–1999 (Table 2) to simulated climate data. This yielded TRGI predictions for periods 1961–1989 and 2041–2060, which correspond to $1 \times CO_2$ and $2 \times CO_2$ scenarios, respectively. The TRGI forecasts show significant growth reductions ($P < 0.01$) under the simulated climate change for *P. banksiana* and *P. tremuloides* (Table 3). The average growth of

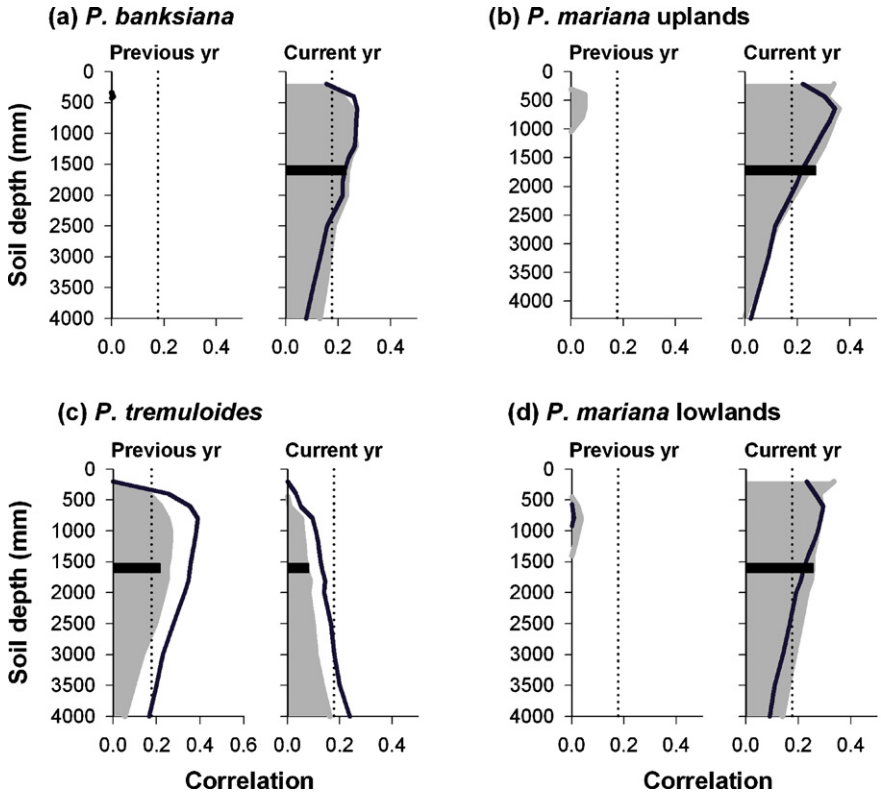

Fig. 5 – Sensitivity analysis of NPP_s to variations in soil depth and period. Starting at 200 mm from the surface and for every 200 mm up to 2000, and then for every 500 mm up to 4000, Spearman rank correlations were computed between actual TRGI and previous year and current year January to December NPP_s (shaded area). (Backward lags of NPP_s were also correlated with the corresponding TRGI in order to account for the lagged response in tree growth.) The black bar marks the correlation between actual TRGI and the average of all NPP_s simulations. Similarly, correlations were computed between NPP_s and TRGI estimates from Fig. 4 (solid lines). The vertical dotted line denotes the one-tailed *p*-value 0.05; a correlation exceeding this line indicates a significant positive relation between NPP_s and TRGI. The interval of analysis was 1912–1999.

P. mariana in a 2 × CO_2 scenario is significantly different from that of the 1 × CO_2 scenario but only in lowland sites ($P = 0.04$) (Table 3); for upland sites the 2 × CO_2 average growth is not significantly different for the reference period ($P = 0.16$). Because the majority of results point in the same direction, we may conclude that the simulated decrease of TRGI in the time slice 2041–2060 is a robust feature. Are these predictions consistent with simulations generated by the growth process-based model?

3.3. *Simulation of future NPP_s*

We first evaluated the performance of the process-based model to adequately simulate NPP_s. Simulations for soil depths ranging from 200 to 4000 mm were conducted over 1912–1999 and each simulation was correlated with observed and estimated TRGI (there are no field data available for rooting depth). Backward lags of NPP_s were also included in the correlation analysis to account for the lagged climate response in TRGI (Girardin and Tardif, 2005). Results (Fig. 5) show significant but low correlations between observed TRGI and simulated NPP_s; the maximum amount of shared variance attained was 13%. The highest correlations were obtained with moderate to deep soil depths for *P. banksiana* (highest correlation at 600–1400 mm), shallow to moderate depths for *P. mariana* (highest at 200 mm for lowlands and 600 mm for uplands), and deep soil depths for *P. tremuloides* (1000 mm during the year previous to ring formation to 4000 mm for the current year). The substitution of observed TRGI with the predicted TRGI (refer to Fig. 4) yielded similar correlograms (Fig. 5). All species under study, with the exception of *P. tremuloides*, are reported as having shallow rooting systems. Much of the root system of *P. banksiana* is reported to be in the upper 150 mm, although a taproot may extend below 2700 mm on well-drained soils (Rudolph and Laidly, 1990). Although some *P. mariana* roots may penetrate to 600 mm, most spread laterally at the moss-humus interface, with the bulk of the root biomass being in the upper 200 mm of the organic horizons (Viereck and Johnston, 1990). For *P. tremuloides*, the fine feeding roots may descend to depths of 3000 mm or more (Perala,

Table 4 – Monthly signs of the temperature, precipitation, and Drought Code Spearman rank correlation coefficients by species, for predicted TRGI and simulated NPP_s (− for negative correlation and + for positive; two-sided 95% significance level)

	Previous year						Current year									
	j	a	s	o	n	d	J	F	M	A	M	J	J	A	S	O
TRGI (Mean temperature)																
P. banksiana	−	−	−					−				−				−
P. mariana uplands		−												+		
P. mariana lowlands	−	−										−				
P. tremuloides	−	−	−					−	−						+	
NPP_s																
P. banksiana							+		+	+	+	+			+	
P. mariana uplands										+	+	+			+	
P. mariana lowlands															+	
P. tremuloides										+	+					
TRGI (precipitation)																
P. banksiana	+	+		−								+		+		
P. mariana uplands	+			−								+				+
P. mariana lowlands	+	+		−								+			+	
P. tremuloides	+	+				+	+									
NPP_s																
P. banksiana											+	+	+	+		
P. mariana uplands				−							+	+	+	+	+	
P. mariana lowlands				−							+	+	+	+	+	
P. tremuloides											+	+	+	+	+	
TRGI (Drought Code)																
P. banksiana		−	−	−								−	−	−	−	
P. mariana uplands		−										−	−	−	−	−
P. mariana lowlands		−	−									−	−	−	−	−
P. tremuloides	−	−	−	−									−			
NPP_s																
P. banksiana										+			−	−	−	
P. mariana uplands												−	−	−	−	−
P. mariana lowlands			−	−								−	−	−	−	−
P. tremuloides				−								−	−	−	−	−

Months previous to the year of ring formation (July–December) are labelled with small caps and those of current year to ring formation (January–October) are labelled with capital letters. Analyses were conducted over the period 1912–1999.

1990). Hence, the maximization of the correlation coefficients using the soil depth parameter (Fig. 5) yields realistic estimates of rooting depth.

The simulations for periods 1961–1989 and 2041–2049 (Fig. 6) indicated increasing yearly NPP_s ($P < 0.01$) in the $2 \times CO_2$ driven climate scenario for coniferous species when providing the model with deep (>2000 mm) soil depths. The increase was marginal for moderate depths (800 to 2000 mm; $P < 0.05$). For shallow soil depths (200 to 600 mm), results indicated a state of 'no significant change' ($P > 0.05$). NPP_s of *P. tremuloides* was also predicted to be higher in the $2 \times CO_2$ scenario (Fig. 6), although the difference in mean was not statistically significant for depths < 2500 mm. Simulation of monthly NPP (Fig. 7) for depths that gave the best correlation with TRGI indicated that for coniferous species, the increase of yearly NPP_s was largely due to enhanced productivity in April. For *P. banksiana*, the gain of NPP during April alone (21.5 g m^{-2} year^{-1}) accounted for 33.1% of the yearly gain (64.9 g m^{-2} year^{-1}). The longer

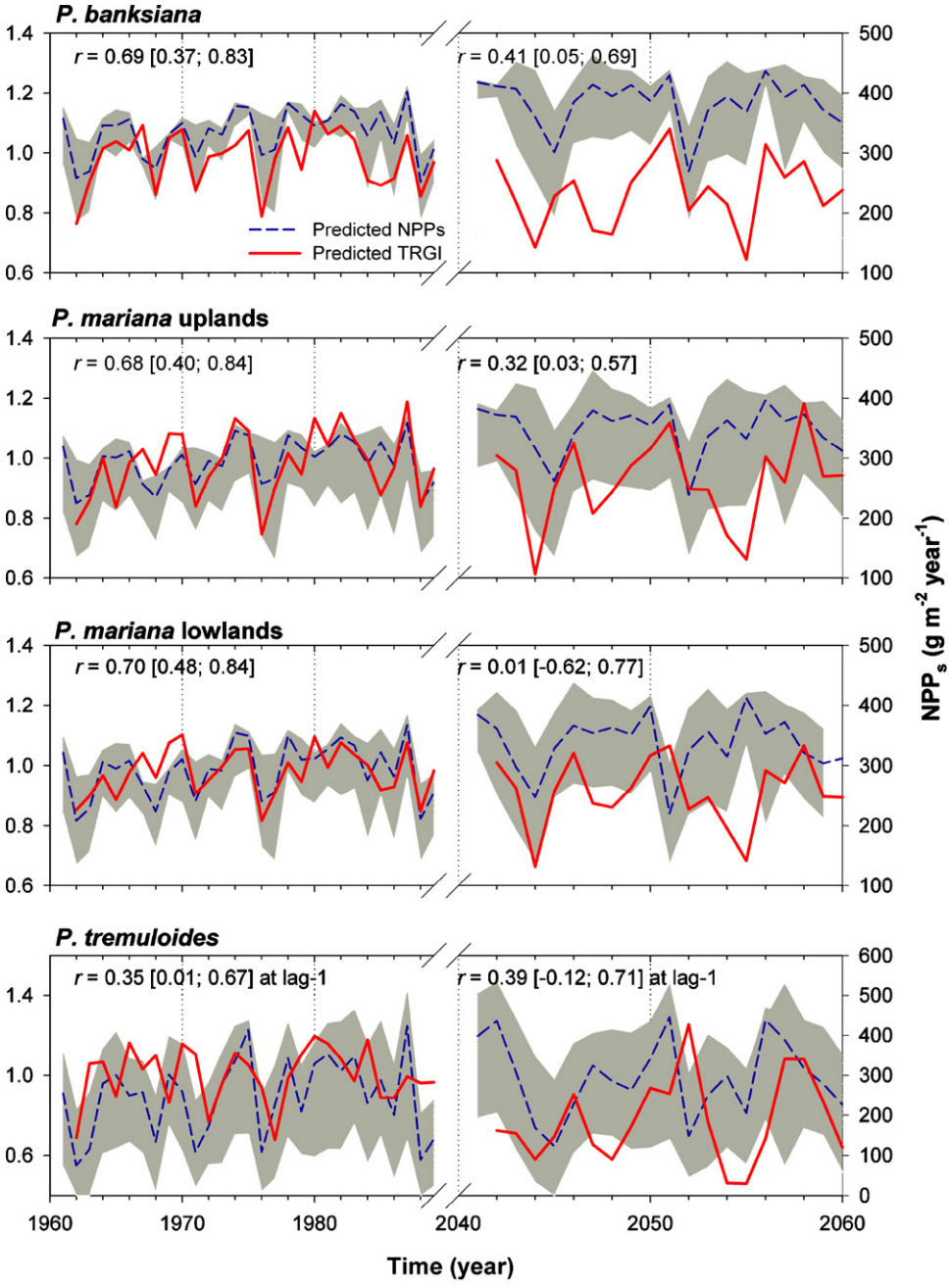

Fig. 6 – Predicted TRGI (solid line) versus average simulated net primary productivity allocated to stem development (NPP_s; dashed line) over horizons 1961–1989 and 2041–2060. The NPP_s simulations were first computed for various soil depths, ranging from 400 mm (least productive stands) to 4000 mm (most productive stands) and then averaged. The grey shaded area delineates the range given by the uppermost and lowermost soil depths. The Pearson correlation *r* with 95% bootstrap confidence interval is the correlation between the average NPP_s and the predicted TRGI for a given time horizon (95% confidence interval accounts for autocorrelation in data; Mudelsee, 2003).

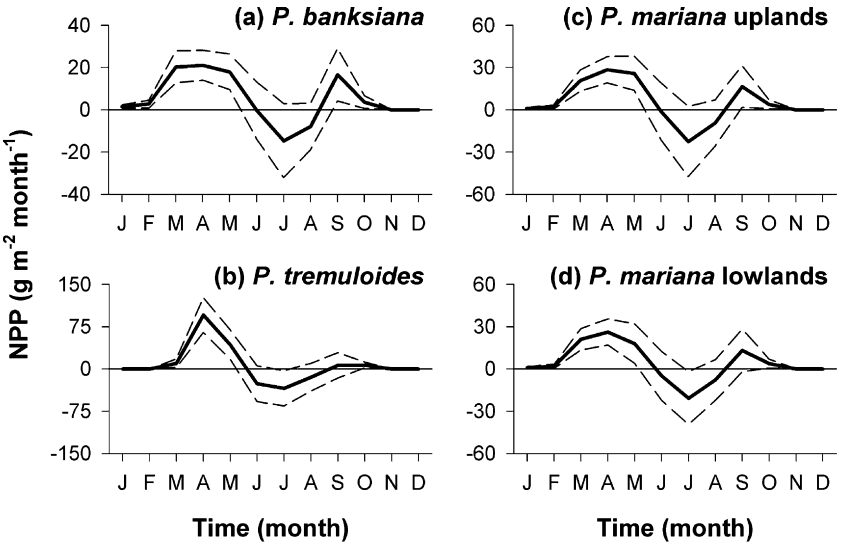

Fig. 7 – Bold lines: average monthly NPP differences between the 2 × CO_2 and 1 × CO_2 driven climate scenarios. The period is January 'J' to December 'D'. Positive values indicate greater NPP in the 2 × CO_2 scenario; negative values indicate greater NPP in the 1 × CO_2 scenario. Dashed lines show the 95% confidence interval: when the zero line crosses the confidence interval, the null hypothesis of 'no significant difference in NPP between scenarios' cannot be rejected at the 95% level. Inputs for soil depths correspond to (a) 800 mm, (b) 1000 mm, (c) 600 mm, and (d) 400 mm.

growing season would benefit evergreen species as indicated by these simulations. Trees growing on shallow soils (depths < 600 mm) may however see this spring gain reduced. An increase in April NPP was also observed with *P. tremuloides* due to an earlier budbreak and was sufficient to compensate for decreasing summertime NPP (Fig. 7). Finally, it is worth mentioning that in addition to changes in mean, all simulations show increased variance around the mean in a

Table 5 – Calibration and verification statistics of TRGI empirical prediction models computed from physiological variables VPD (vapour pressure deficit) and NPP (net primary productivity) at times of storage (st) and growth (gr); + and − indicate the sign of coefficients

	P. banksiana	*P. mariana* uplands	*P. mariana* lowlands	*P. tremuloides*
Calibration 1912–1999				
R^2	0.256	0.331	0.240	0.212
Adjusted r^2	0.238	0.307	0.222	0.193
Standard error of the estimate	0.117	0.112	0.101	0.152
Parameters	$-VPD_{st} + NPP_{gr}$	$-VPD_{st} + NPP_{gr} - VPD_{gr}$	$-VPD_{st} + NPP_{gr}$	$NPP_{st} - VPD_{st}$
Calibration 1912–1969				
R^2	0.249	0.304	0.193	0.180
Adjusted r^2	0.221	0.265	0.164	0.150
Standard error of the estimate	0.117	0.112	0.096	0.170
Verification 1970–1999				
Correlation (r^2)[a]	0.245[a]	0.297[a]	0.343[a]	0.276[a]
Reduction of error (RE)[b]	0.206[b]	0.323[b]	0.229[b]	0.274[b]
Product mean test (PM)[c]	2.031[c]	2.675[c]	2.537[c]	3.194[c]
2 × CO_2/1 × CO_2	0.97[*]	0.88[**]	0.95[**]	0.88[**]

Ratios of average TRGI for 2 × CO_2/1 × CO_2 scenarios are also shown. Soil depths used for NPP computation correspond to 800, 600, 400, and 1000 mm.

[a] Significant at $p < 0.05$ if r^2 (r square) > 0.10.

[b] Considered satisfactory if RE > 0. Whenever RE is greater than zero, the prediction is considered as being a better estimate of growth than the calibration period mean.

[c] Considered significant at $p < 0.05$ if PM > 1.70. A significant PM test result indicates that the magnitude and the direction of year-to-year changes are statistically significant.

[*] Significant at $p < 0.10$.

[**] Significant at $p < 0.05$.

changing climate (i.e. greater year-to-year variability of NPP_s; Fig. 6).

Results from simulations of climate change impacts on stem development differ between the two modelling approaches. Results from the empirical modelling approach indicate (in terms of statistical significance) negative or neutral impacts of climate change on growth, while results from the process-based approach suggested a beneficial or neutral effect, depending on species and the assumed depth of soil. Intriguingly, a comparison of the simulations indicated strong coherence between the modelling results of coniferous species in the $1 \times CO_2$ scenario (Fig. 6). The discrepancy would therefore suggest that one approach is either not sensitive or too sensitive to changes in the mean state of the climate. Correlation analysis with monthly climate variables (temperature, precipitation, and Drought Code; Table 4) revealed that both predicted TRGI and simulated NPP_s were sensitive to drought and precipitation variability. The most discernable cause of discrepancy emerged with the response to temperature: NPP_s simulations showed highly pronounced correlations with spring and early fall temperatures, a signal not well reflected in TRGI estimates (Table 4). Additionally,

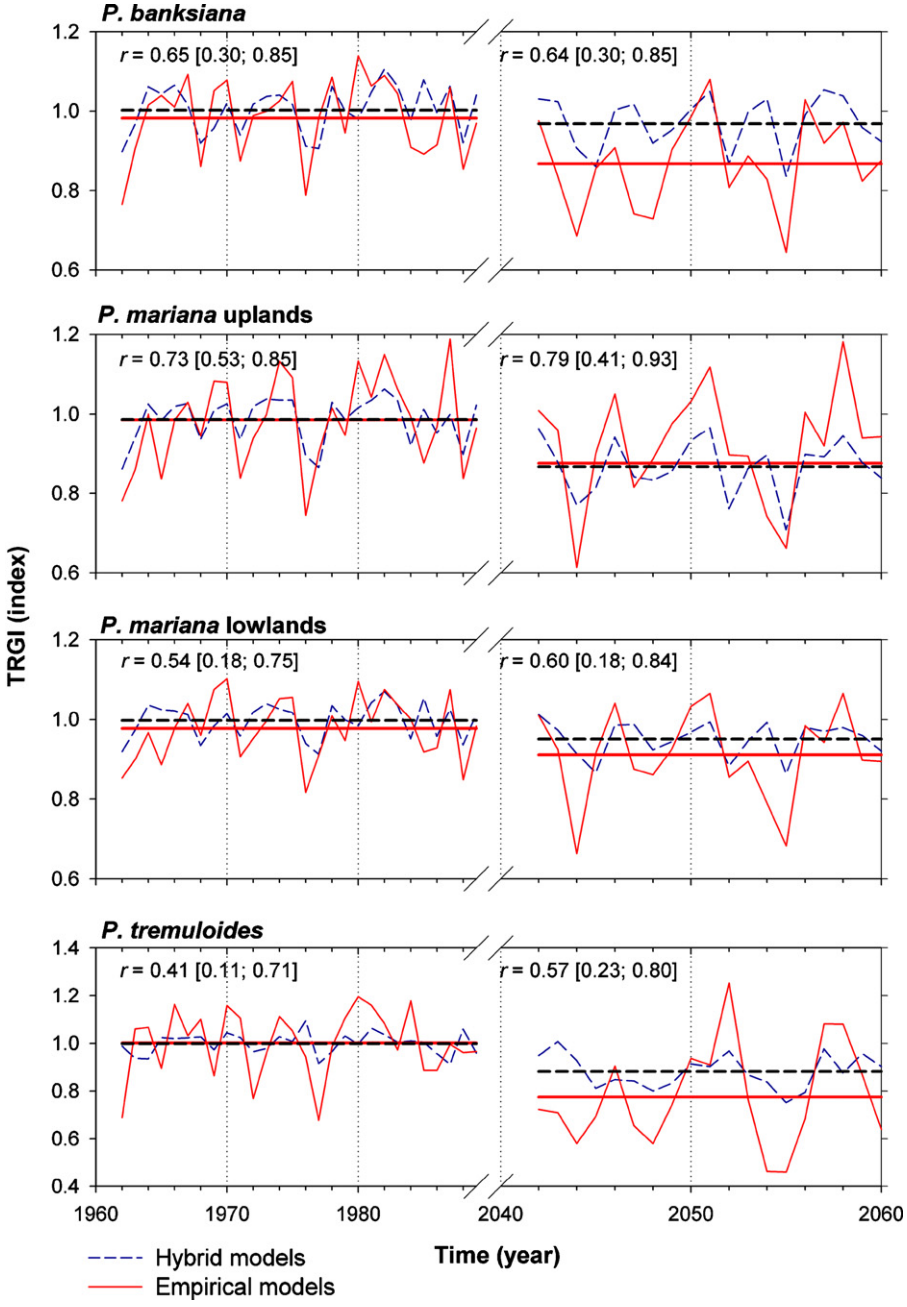

Fig. 8 – Predicted TRGI obtained from the empirical (solid line) and hybrid (dashed line) modelling approaches over horizons 1961–1989 and 2041–2060. Horizontal bold lines show averages over both time horizons. Inputs for soil depths correspond to (a) 800 mm, (b) 600 mm, (c) 400 mm, and (d) 1000 mm. The Pearson correlation *r* with 95% bootstrap confidence interval is shown for both horizons.

TRGI estimates of coniferous species showed negative correlations to warm season temperatures during the year previous to ring formation. A negative correlation to spring temperature is also unique to TRGI estimates of *P. tremuloides* (Table 4). Hence, it appears that the cause of discrepancies is related to a greater sensitivity of NPP_s simulations to growing season length and a weaker response of NPP_s simulations to warm season temperatures. In the following section, we try to bridge the gap between the two modelling approaches.

3.4. *Hybrid modelling approach*

Least-squares stepwise multiple regression employing a backward selection (Eq. (2)) was used to calibrate TRGI of all three species against their respective total NPP obtained from StandLEAP (under the optimized soil depths) and average VPD during the years previous (July to December) and current (January to July) to ring formation in order to account for lagged effects in TRGI. These regression models are therefore limited to a potential of only four predictor variables. We focussed on VPD as a potential source of discrepancy between models because verification of the process-based approach had revealed weaknesses with respect to this variable in the original datasets used for FineLEAP calibration. Additionally, changes in carbon allocated to stem growth under a changing climate were coarsely estimated by multiplying the $2 \times CO_2/1 \times CO_2$ TRGI ratio (and standard error; Table 5) by the average NPP_s of the $1 \times CO_2$ time horizon (under optimal soil depths; Fig. 6).

The results indicate that up to 33% of the variance in *P. mariana* growth, 21% in *P. tremuloides*, and 25% in *P. banksiana* could be accounted for by two or three predictor variables (Table 5). All four models have significant predictive skills. Consistent with former empirical results, predictions of climate change impacts show decreasing radial growth ($P < 0.05$) in the $2 \times CO_2$ climate scenario (Table 5; Fig. 8). The most important reduction in the amount of carbon allocated to stem growth is found with *P. mariana* from upland sites: a decrease of 31.7 $g\,m^{-2}\,year^{-1}$ is projected (264.0–232.3 ($\pm$29.6) $g\,m^{-2}\,year^{-1}$). The reduction in *P. tremuloides* is estimated at 27.4 $g\,m^{-2}\,year^{-1}$ (205.6–180.9 ($\pm$31.3) $g\,m^{-2}\,year^{-1}$) and that of *P. banksiana* at 9.5 $g\,m^{-2}\,year^{-1}$ (318.2–308.7 ($\pm$37.2) $g\,m^{-2}\,year^{-1}$). The reduction in *P. mariana* growing on lowland sites is estimated at 11.0 $g\,m^{-2}\,year^{-1}$ (219.4–208.4 ($\pm$22.2) $g\,m^{-2}\,year^{-1}$). Results obtained in this manner are similar and well correlated to those obtained using a much larger suite of variables (Fig. 8) and suggest that, for the DMPF, the positive effect of increasing growing season length would be counteracted by increasing summer temperatures. This trend is not as clear for *P. tremuloides* as it is for the other two species, given that there are no growth predictors representative of its spring phenology in the empirical and hybrid models (see Tables 2, 4 and 5).

4. Discussion

Our results show that robust TRGI prediction models can be developed for radial growth forecasts in Canadian boreal forests. All three empirical models of coniferous TRGI meet the statistical requirements of temporal stability in tree growth and climate relationships. Only the hardwood TRGI model does not satisfy the stability requirement. However, the extrapolation of modelled relationships in a climate change scenario yields results that, in terms of statistical significance, diverge from simulations obtained with a canopy-level process-based model. Indeed, the results from the former approach suggest no beneficial effect of climate change on tree radial growth (as defined by CGCM2 GHG+A IPCC B2 scenario run). In contrast, the latter approach shows that the impact of an increased drought stress, which reduces NPP in summertime, could be compensated for and overwhelmed by enhanced productivity in spring. As discussed below, there are a number of uncertainties in the input processes in both empirical and process-based model approaches that still need to be addressed. The hybrid modelling approach appears to address some of these limitations.

Empirical models are usually specific to the site and conditions of measurements used to determine parameter values and they lack the capacity to extrapolate to regions and conditions that are significantly different (Landsberg, 2003b). It is for instance not recommended to use a model outside of its calibration range without proper verification (Robinson and Ek, 2000). In this regard, the outcome from the empirical modelling approach contains uncertainties: the climate in the $2 \times CO_2$ horizon is significantly different from that of the $1 \times CO_2$ horizon (Fig. 2). The predictive skills of the coniferous TRGI models are significant over the current climate, but may not be so in a changing climate. In addition, tree-growth and climate relations are most often considered linear, which may be inconsistent with the notion of physiological optimum for tree growth, i.e. where maximum growth occurs in an intermediate climate condition (Kramer and Kozlowski, 1979; Woodhouse, 1999; Fritts, 2001; D'Arrigo et al., 2004).

The performance of the empirical model also depends largely on the absence of external forcing (or noise) that can weaken or alter the climate signal in TRGI. These forcings include insect herbivory, fire disturbances, and/or the effect of intra- and inter-species competition (Zahner, 1968; Fritts, 2001; Girardin et al., 2001; Hogg et al., 2005; Sutton and Tardif, 2007). In fact, insect herbivory is perhaps one reason why the empirical model for *P. tremuloides* had lower predictive skills. The reduction in the expression of climate signals in the TRGI of *P. tremuloides* due to defoliation by the forest tent caterpillar (*Malacosoma disstria* Hubner) is now well documented. Major defoliation by the forest tent caterpillar can lead to significant growth reductions (Sutton and Tardif, 2005, 2007) and, in some instances, can account for more temporal variation in stem-area increment than any of the variables describing climate variation (Hogg et al., 2005). That said, there is no clear evidence that the presence of defoliation in calibration of TRGI altered the forecasts. Indeed, removal of major forest tent caterpillar episodes (reported by Sutton and Tardif, 2007) from the period withheld for calibration of the TRGI model did not lead to different projections of climate change impacts (results not shown). Nonetheless, the distortion effect combined with the non-linear processes affecting forest productivity are of sufficient concern to justify the development of process-based models that can predict tree growth with a higher degree of certainty.

The statistical comparison of TRGI and NPP_s time series made it possible to cross-validate the StandLEAP model's capacity to capture interannual variation in stem increment. Although conclusive, the results showed that the process-based model did lack some climate sensitivity. The significance of VPD in addition to the process-based-derived NPP in a fit to TRGI data (via the hybrid modelling approach) suggested that the full impact of this variable, or of other environmental conditions that are well correlated with VPD, were not well captured in the process-based model. Another source of uncertainty in the simulations was the general lack of information on soil depths (rooting extension) and soil texture, two variables that are needed to generate good estimates of soil water-holding capacity (Hall et al., 2006). Coops and Waring (2001) have shown that 3-PG accurately differentiates rates of soil water depletion once a good estimate of soil water-holding capacity can be obtained. This weakness appears critical in a climate change simulation. Simulation results show that minor variations in soil water-holding capacity through modification of soil depths yield a range of outcomes and a large influence on the rejection or not of the null hypothesis. The rooting depth is a vexing question as field observation of roots can never account for the actual capacity of trees to extract water from a soil profile. We propose that modelling approaches like the one illustrated in Fig. 5 are likely the best sources of information regarding values of rooting depth to be used in models, realizing that models are by their very nature a simplified representation of reality. In another approach, Bernier et al. (2006) looked at the mass balance of water in the soil in comparison with measured transpiration losses for the estimation of rooting depth for *P. tremuloides* and *P. banksiana*. In both cases, the approaches yielded results that were in a range of realistic values.

Therefore, we propose that the use of a hybrid modelling approach, in which growth variables predicted by a process-based model are used within empirical equations of TRGI, offers three significant advantages compared with purely empirical models. The first is to improve the sensitivity of the tree growth forecasts to climate variability. The second is that process-based models can take into account non-linear processes affecting NPP_s. For this reason, the predictions in a changing climate are less likely to be biased than those obtained from an empirical model calibrated on monthly climate data alone. Thirdly, use of the hybrid approach may reduce the number of predictor variables in TRGI equations without sacrificing the predictive ability of the empirical model. Our simulation of *P. tremuloides* TRGI is a good example of this last point with the 13 variables required in the empirical approach replaced by only two variables in the hybrid approach, and the latter approach yielding a better fit to the data from the verification period (compare Tables 2 and 5).

Finally, additional gains in the performance of the process-based and hybrid modelling approaches could be made with the acquisition of information on the phenology of species and the timing of carbon allocation to stem growth and cell production (Tardif et al., 2001b; Deslauriers and Morin, 2005; Rossi et al., 2006; Ko Heinrichs et al., 2007). In a number of bioclimatic models, carbon allocation to stem development is restricted to the period of growth usually defined as between the end of leaf out and the end of summer. For means of simplicity, the process of carbon storage and mobilization is not represented in StandLEAP. Together with allocation to all other tree components, NPP_s is computed as a fraction of NPP that is determined on a yearly basis (default from January to December) based on allometric rules. However, many tree-ring studies suggest that late season photosynthesis produces assimilates that are used for stem growth in the following year (Foster and LeBlanc, 1993; Graumlich, 1993; Tardif and Bergeron, 1997; Fritts, 2001; Tardif et al., 2001a; Misson, 2004; Girardin and Tardif, 2005; Rathgeber et al., 2005; Kagawa et al., 2006). The importance of this lagged effect is also supported by our results, with the selection in the hybrid models of TRGI of growth predictors from the year previous to ring formation (Table 5). Furthermore, other studies suggest that while metabolic activities during cell formation are allowed and maintained by weather, the signal regulating the timing of growth rate could be related to photoperiod (i.e. Rossi et al., 2006). Useful information for generating allometric rules defining carbon storage and mobilization could be explored through the separation of earlywood and latewood production because of the specificity of each process to climatic influences (Rathgeber et al., 2000, 2003; Misson et al., 2004; Tardif and Conciatori, 2006). Information specifically related to stem growth and cell production could be gained with the use of an index of wood increment combining both tree-ring width and tree-ring density measurements (see Rathgeber et al., 2000, 2003; Misson et al., 2004). Detailed information on cambium activity and wood formation could also be gained with repeated microcore sampling during the growing season (Mäkinen et al., 2003; Deslauriers and Morin, 2005; Rossi et al., 2006; Ko Heinrichs et al., 2007). Pulse-labeling of saplings and trees with $^{13}CO_2$ could also help to clarify the seasonal course of carbon allocation patterns among needles, branches, stem and roots (Kagawa et al., 2006).

5. Conclusion

We used three modelling approaches for predicting tree growth of *P. banksiana*, *P. mariana* and *P. tremuloides* in the DMPF in a climate change scenario (GHG + A IPCC B2 scenario run):

(1) In the empirical modelling approach, we used least-squares regression to calibrate TRGI against monthly climate data. After development of the empirical models of TRGI and verification of their predictive skills, the regression coefficients estimated for the calibration period were applied to simulated climate data ($1\times$ and $2\times CO_2$ scenarios) and prediction of future TRGI was made.
(2) A process-based productivity model was used to produce estimates of NPP that served as a direct link between the climate scenario and the production of wood fibre. We used a two-level scaling approach to achieve estimates of NPP. At the finest scale, a leaf-level model of photosynthesis (FineLEAP) was used to simulate canopy properties per species and their interaction with the variability in radiation, temperature and vapour pressure deficit. Then, a top-down plot-level model of forest productivity (StandLEAP) was used to simulate landscape-level productivity by capturing the between-stand variability in forest cover.

The two levels of simulation were linked functionally as parameters of the coarser models were estimated from simulation results of the finer models.

(3) As we found that both empirical and process-based model approaches had weaknesses, a hybrid model approach was developed by incorporating the environmental variability collected by the process-based model into empirical equations of TRGI.

The results from the empirical and hybrid modelling of TRGI have shown that the two approaches can yield robust estimates of TRGI over the current climate. The prospect of climate change in the boreal forest is often associated with increased growth of the forest. The results from these latter approaches suggested otherwise for the DMPF: all three species under study showed no beneficial effect of climate change on tree radial growth.

Notwithstanding all of the above discussion on caveats to modelling approaches, uncertainties could be overshadowed by other processes involved in the control of tree growth and NPP_s. Neither of the modelling approaches presented in this study considered CO_2 enrichment effects and nitrogen cycle on tree growth and effects of stand disturbances (insect and fire) on tree mortality, stem recruitment, changes in hydrology and nutrient recycling. Direct effects of atmospheric CO_2 increase with carbon storage and tree growth may occur through photosynthesis and water use efficiency linked to stomatal permeability (Bonan, 2002; Kienast and Luxmoore, 1988; Rathgeber et al., 2000). Additionally, NPP is closely related to fire disturbance regimes (Coursolle et al., 2006). Fire activity is predicted to increase significantly in the DMPF and surrounding areas (Flannigan et al., 2005; Girardin and Mudelsee, in press) and this will affect stand age distribution and hence NPP (Peng and Apps, 1999). Omission of information on disturbance may hence invalidate prediction of climate change impacts on tree and species productivity (Weber and Flannigan, 1997). Significant information on this matter could be gained with the modelling of NPP_s for a range of stand age cohorts obtained from a dendroecological fire history reconstruction of the DMPF (Tardif, 2004). Such a contribution to a dynamic vegetation – climate – disturbance model will help us to better describe the potential impacts of climate change and to explore adaptation strategies for sustainable management planning under climate change.

Acknowledgements

This work was made possible in part by a post-doctoral scholarship from the Natural Sciences and Engineering Research Council of Canada to the lead author. We thank the Canadian Centre for Climate Modelling and Analysis (CCCma; a division of the Climate Research Branch of the Meteorological Service of Canada) for providing the climate simulations and the Meteorological Service of Canada for providing the instrumental climate data. We thank Xiao Jing Guo for her help with the process-based model. We thank Chhun-Huor Ung, two anonymous reviewers, and Pamela Cheers for comments and the reviewing of the manuscript.

Appendix A

See Tables A1 and A2.

Table A1 – Standardized TRGI statistics

	P. banksiana	*P. tremuloides*	*P. mariana* uplands	*P. mariana* lowlands
Chronology length	1717–2001	1806–2001	1724–2000	1758–2001
Number of trees	291	194	11	33
Number of radii	521	264	19	64
Percentage of absent rings	0.12	0.27	0.07	0.12
Mean sensitivity	0.13	0.23	0.13	0.11
Standard deviation	0.17	0.29	0.17	0.16
First-order autocorrelation	0.58	0.56	0.55	0.63
Common interval analysis (1945–1999)				
Number of trees	25	36	10	26
Number of radii	43	46	16	45
Variance in first PCA vector (%)	30.52	35.31	36.94	29.49
Expressed population signal	0.90	0.95	0.77	0.89
Intercore correlation	0.27	0.32	0.28	0.25
Intertree correlation	0.26	0.32	0.26	0.24
Intratree correlation	0.59	0.67	0.67	0.52

Table A2 – Parameters and allometric coefficients used in program StandLEAP

Abbreviations	Parameters	*P. banksiana*	*P. mariana*	*P. tremuloides*
Tree-level allocation model parameters				
folPra	Allometric coefficient relating foliage biomass and dbh	0.01	0.05	0.02
folPrn	Allometric coefficient relating foliage biomass and dbh	2.34	1.88	1.63
Plot-level allocation model parameters				
folPraM	Allometric coefficient relating foliage biomass to crown biomass	0.82	0.45	0.12
folPrnM	Allometric coefficient relating foliage biomass to crown biomass	0.93	1.00	1.00
stemPra	Allometric coefficient relating stem biomass to aboveground biomass	0.60	0.42	0.68
stemPrn	Allometric coefficient relating stem biomass to aboveground biomass	1.03	1.06	1.02
rootPra	Allometric coefficient relating coarse root biomass to aboveground biomass	1.40	0.29	0.23
rootPrn	Allometric coefficient relating coarse root biomass to aboveground biomass	0.79	0.98	0.96
crownPra	Allometric coefficient relating crown biomass to aboveground biomass	2.01	1.92	0.57
crownPrn	Allometric coefficient relating crown biomass to aboveground biomass	0.76	0.80	0.88
Tree-level allocation model parameters				
abvGndPra	Allometric coefficient relating aboveground biomass and dbh	0.07	0.14	0.08
abvGndPrn	Allometric coefficient relating aboveground biomass and dbh	2.49	2.26	2.48
stemSapwoodPra	Allometric coefficient of living aboveground woody biomass	0.01	0.03	0.02
stemSapwoodPrn	Allometric coefficient of living aboveground woody biomass	2.69	2.58	2.84
fineRtFolRatio	Fine root foliage ratio	0.68	1.33	0.26
Epsilon and water use efficiency model parameters				
beT	Parameter β_l for the epsilon temperature modifier	0.36	0.47	0.25
beqT	Parameter β_q for the epsilon temperature modifier	−0.19	−0.16	−0.25
Tmoy	Parameter β_m for the epsilon temperature modifier	13.33	13.34	13.32
VPDmoy	Parameter for the epsilon vapour pressure deficit modifier	0.65	0.65	0.65
beV	Parameter β_l for the epsilon VPD modifier	0.00	0.00	0.00
beqV	Parameter β_q for the epsilon VPD modifier	0.00	0.00	0.00
epsilonMoy	Average quantum efficiency (mol C (mol photon)$^{-1}$)	0.02	0.02	0.02
beL	Parameter β_l for the epsilon leaf area index modifier	0.35	0.65	0.00
beqL	Parameter β_q for the epsilon leaf area index modifier	−0.17	−0.19	0.00
LAImoy	Parameter β_m for the epsilon leaf area index modifier	5.00	5.00	5.00
PARmoy	Parameter β_m for the epsilon PAR modifier	1036.89	1047.31	1046.73
bwL	Parameter β_l for the water use efficiency—leaf area index modifier	0.00	0.00	−0.73
bwqL	Parameter β_q for the water use efficiency—leaf area index modifier	0.00	0.00	0.52
bwV	Parameter β_l for the water use efficiency—vapour pressure deficit modifier	0.78	0.92	0.78
WUEmoy	Average water use efficiency (mol CO_2/mol H_2O/kPa)	0.00	0.00	0.00
beClim	Parameter β_l for mortality model climate modifier	1.27	0.82	0.00
beqClim	Parameter β_q for mortality model climate modifier	0.00	−0.90	0.00
climMoy	Parameter β_m for mortality model climate modifier	0.72	0.53	0.88
beIw	Parameter β_l for mean ratio of above ground mass increment over above ground mass	0.00	−5.64	0.00
beqIw	Parameter β_q for mean ratio of above ground mass increment over above ground mass	0.00	3.02	0.00
Ingrowth model parameters				
extCoeff_k0	Parameter of the relationship between the extinction coefficient and leaf area index	0.75	0.67	0.66
extCoeff_k1	Parameter of the relationship between the extinction coefficient and leaf area index	−0.25	−0.22	−0.22
GDDFolStart	Degree-days (0 °C) to bud break	116.00	300.00	120.00
GDDFolEnd	Degree-days to end of leaf expansion	766.66	800.00	180.00
GDDFolLowBase	Lower base temperature for growing degree-days sum	2.90	0.00	5.00
folReten	Mean foliage retention time (number of growing seasons)	10.18	8.62	1.00
senescStart	Julian day when leaf fall is allowed to start	270.00	270.00	270.00
propNPP	Proportion between NPP and GPP	0.39	0.34	0.44

REFERENCES

Aber, J.D., Federer, C.A., 1992. A generalized, lumped-parameter model of photosynthesis, evapotranspiration and net primary production in temperate and boreal forest ecosystems. Oecologia 92, 463–474.

Aber, J.D., Ollinger, S.V., Federer, C.A., Reich, P.B., Goulden, M.L., Kicklighter, D.W., Melillo, J.M., Lathrop Jr., R.G., 1995. Predicting the effects of climate change on water yield and forest production in the northeastern United States. Clim. Res. 5, 207–222.

Arbaugh, M.J., Peterson, D.L., 1989. Variable selection in dendroclimatology: an example using simulated tree-ring series. For. Sci. 35, 294–302.

Baldwin, V.C., Burkhart, H.E., Westfall, J.A., Peterson, K.D., 2001. Linking growth and yield and process models to estimate impact of environmental changes on growth of loblolly pine. For. Sci. 47, 77–82.

Bernier, P.Y., Raulier, F., Stenberg, P., Ung, C.H., 2001. Importance of needle age and shoot structure on canopy net photosynthesis of balsam fir (*Abies balsamea*): a spatially inexplicit modeling analysis. Tree Physiol. 21, 815–830.

Bernier, P.Y., Bréda, N., Granier, A., Raulier, F., Mathieu, F., 2002. Validation of a canopy gas exchange model and derivation of a soil water modifier for transpiration for sugar maple (*Acer saccharum* Marsh) using sap flow density measurements. For. Ecol. Manag. 163, 185–196.

Bernier, P.Y., Bartlett, P., Black, T.A., Barr, A., Kljun, N., McCaughey, J.H., 2006. Drought constraints on transpiration and canopy conductance in mature aspen and jack pine stands. Agric. For. Meteorol. 140, 64–78.

Boer, G.J., Flato, G., Ramsden, D., 2000a. A transient climate change simulation with greenhouse gas and aerosol forcing: projected climate to the 21st century. Clim. Dyn. 16, 427–450.

Boer, G.J., Flato, G., Reader, M.C., Ramsden, D., 2000b. A transient climate change simulation with greenhouse gas and aerosol forcing: experimental design and comparison with the instrumental record for the 20th century. Clim. Dyn. 16, 405–425.

Bonan, G., 2002. Ecological Climatology: Concepts and Applications. Cambridge University Press, New York, NY, USA, 678 pp.

Chen, J.M., 1996. Optically-based methods for measuring seasonal variation of leaf area index in boreal conifer stands. Agric. For. Meteorol. 80, 135–163.

Chuine, I., 2000. A unified model for budburst of trees. J. Theor. Biol. 207, 337–347.

Chuine, I., Beaubien, E.G., 2001. Phenology is a major determinant of tree species range. Ecol. Lett. 4, 500–510.

Cook, E.R., Peters, K., 1981. The smoothing spline: a new approach to standardizing forest interior tree-ring width series for dendroclimatic studies. Tree-Ring Bull. 41, 45–53.

Cook, E.R., Holmes, R., 1986. Guide for Computer Program ARSTAN. Laboratory of Tree-Ring Research, University of Arizona, Tucson, Arizona, 51 pp.

Cook, E.R., Kairiukstis, L.A., 1990. Methods of Dendrochronology: Applications in the Environmental Sciences. Kluwer Academic Publishers, Boston, MA, USA, 408 pp.

Cook, E.R., Briffa, K.R., Jones, P.D., 1994. Spatial regression methods in dendroclimatology: a review and comparison of two techniques. Int. J. Climatol. 14, 379–402.

Coops, N.C., Waring, R.H., 2001. Estimating forest productivity in the eastern Siskiyou Mountains of southwestern Oregon using a satellite driven process model, 3-PGS. Can. J. For. Res. 31, 143–154.

Coursolle, C., Margolis, H.A., Barr, A.G., et al., 2006. Late-summer carbon fluxes from Canadian forests and peatlands along an east–west continental transect. Can. J. For. Res. 36, 783–800.

Dang, Q.L., Margolis, H.A., Sy, M., Coyea, M.R., Collatz, G.J., Walthall, C.L., 1997. Profiles of photosynthetically active radiation, nitrogen and photosynthetic capacity in the boreal forest: implications for scaling from leaf to canopy. J. Geophys. Res. 102 (D24), 28845–28859.

Dang, Q.L., Margolis, H.A., Collatz, G.J., 1998. Parameterization and testing of a coupled photosynthesis-stomatal conductance model for boreal trees. Tree Physiol. 18, 141–153.

D'Arrigo, R.D., Kaufmann, R.K., Davi, N., Jacoby, G.C., Laskowski, C., Myneni, R.B., Cherubini, P., 2004. Thresholds for warming-induced growth decline at elevational tree line in the Yukon Territory, Canada. Global Biogeochem. Cycles 18, GB3021, doi:10.1029/2004GB002249.

Deslauriers, A., Morin, H., 2005. Intra-annual tracheid production in balsam fir stems and the effect of meteorological variables. Trees-Struct. Funct. 19, 402–408.

Draper, N.R., Smith, H., 1998. Applied Regression Analysis, 3rd ed. Wiley, New York, 706 pp.

Ecological Stratification Working Group, 1996. A National Ecological Framework for Canada. Agriculture and Agri-Food Canada and Environment Canada, Ottawa, 125 pp.

Environment Canada, 2000. Canadian Daily Climate Data: Temperature and Precipitation. Meteorological Service of Canada, Climate Monitoring and Data Interpretation Division of the Climate Research Branch, Downsview, Ontario, Canada.

Farquhar, G.D., Von Caemmerer, S., Berry, J.A., 1980. A biochemical model of photosynthetic CO_2 assimilation in leaves of C_3 species. Planta 149, 78–90.

Flannigan, M.D., Logan, K.A., Amiro, B.D., Skinner, W.R., Stocks, B.J., 2005. Future area burned in Canada. Clim. Change 72, 1–16.

Flato, G.M., Boer, G.J., Lee, W.G., McFarlane, N.A., Ramsden, D., Reader, M.C., Weaver, A.J., 2000. The Canadian Centre for Climate Modelling and Analysis global coupled model and its climate. Clim. Dyn. 16, 451–467.

Flato, G.M., Boer, G.J., 2001. Warming asymmetry in climate change simulations. Geophys. Res. Lett. 28, 195–198.

Foster, J.R., LeBlanc, D.C., 1993. A physiological approach to dendroclimatic modeling of oak radial growth in the midwestern United States. Can. J. For. Res. 23, 783–798.

Fournier, R.A., Rich, P.M., Landry, R., 1997. Hierarchical characterization of canopy architecture for boreal forest. J. Geophys. Res. 102 (24), 29445–29454.

Fritts, H.C., 2001. Tree Rings and Climate. Blackburn Press, Caldwell, NJ, USA, 567 pp.

Girardin, M.P., Mudelsee, M., in press. Past and future changes in Canadian boreal wildfire activity. Ecol. Appl.

Girardin, M.P., Tardif, J., 2005. Sensitivity of tree growth to the atmospheric vertical profile in the Boreal Plains of Manitoba, Canada. Can. J. For. Res. 35, 48–64.

Girardin, M.P., Tardif, J., Bergeron, Y., 2001. Radial growth analysis of *Larix laricina* from the Lake Duparquet area, Quebec, in relation to climate and larch sawfly outbreaks. Ecoscience 8, 127–138.

Girardin, M.P., Tardif, J., Flannigan, M.D., Wotton, B.M., Bergeron, Y., 2004. Trends and periodicities in the Canadian Drought Code and their relationships with atmospheric circulation for the southern Canadian boreal forest. Can. J. For. Res. 34, 103–119.

Girardin, M.P., Tardif, J.C., Flannigan, M.D., Bergeron, Y., 2006. Synoptic-scale atmospheric circulation and boreal Canada summer drought variability of the past three centuries. J. Clim. 19, 1922–1947.

Gower, S.T., Vogel, J.G., Norman, J.M., Kucharik, C.J., Steele, S.J., Stow, T.K., 1997. Carbon distribution and aboveground net

primary production in aspen, jack pine, and black spruce stands in Saskatchewan and Manitoba, Canada. J. Geophys. Res. 102 (24), 29029–29042.
Graumlich, L.J., 1993. Response of tree growth to climatic variation in the mixed conifer and deciduous forests of the upper Great Lakes region. Can. J. For. Res. 23, 133–143.
Hall, R.J., Raulier, F., Price, D.T., Arsenault, E., Bernier, P.Y., Case, B.S., Guo, X., 2006. Integrating remote sensing and climate data with process-based models to map forest productivity within west-central Alberta's boreal forest: Ecoleap-West. For. Chron. 82, 159–176.
Hänninen, H., 1990. Modelling bud dormancy release in trees from cool and temperate regions. Acta For. Fenn. 213, 1–47.
Hofgaard, A., Tardif, J., Bergeron, Y., 1999. Dendroclimatic response of *Picea mariana* and *Pinus banksiana* along a latitudinal gradient in the eastern Canadian boreal forest. Can. J. For. Res. 29, 1333–1346.
Hogg, E.H., 1994. Climate and the southern limit of the western Canadian boreal forest. Can. J. For. Res. 24, 1835–1845.
Hogg, E.H., Bernier, P.Y., 2005. Climate change impacts on drought-prone forests in western Canada. For. Chron. 81, 675–682.
Hogg, E.H., Brandt, J.P., Kochtubajda, B., 2005. Factors affecting interannual variation in growth of western Canadian aspen forests during 1951–2000. Can. J. For. Res. 35, 610–622.
Holmes, R.L., 1999. Dendrochronology Program Library. Laboratory of Tree-Ring Research, University of Arizona, Tucson, Arizona.
Hunt Jr., E.R., Martin, F.C., Running, S.W., 1991. Simulating the effects of climate variation on stem carbon accumulation of a ponderosa pine stand: comparison with annual growth increment data. Tree Physiol. 9, 161–171.
Kagawa, A., Sugimoto, A., Maximov, T.C., 2006. $^{13}CO_2$ pulse-labelling of photoassimilates reveals carbon allocation within and between tree rings. Plant Cell Environ. 29, 1571–1584.
Kenkel, N., Hamel, C., 2000. Structure and Dynamics of Boreal Forest Stands in the Duck Mountains, Manitoba. Sustainable Forest Management Network. Project Reports 2000 Series. University of Alberta, Edmonton, Alberta, 54 pp.
Kienast, F., Luxmoore, R.J., 1988. Tree-ring analysis and conifer growth responses to increased atmospheric CO_2 levels. Oecologia 76, 487–495.
Kleidon, A., Heimann, M., 1998. A method of determining rooting depth from a terrestrial biosphere model and its impacts on the global water and carbon cycle. Global Change Biol. 4, 275–286.
Ko Heinrichs, D., Tardif, J.C., Bergeron, Y., 2007. Xylem production in six tree species growing on an island in the boreal forest region of western Quebec, Canada. Can. J. Bot. 85, 518–525.
Kramer, P., Kozlowski, T., 1979. Physiology of Woody Plants. Academic Press, San Diego, CA, USA.
Lambert, M.C., Ung, C.H., Raulier, F., 2005. Canadian national tree aboveground biomass equations. Can. J. For. Res. 35, 1996–2018.
Landsberg, J., 2003a. Modelling forest ecosystems: state of the art, challenges, and future directions. Can. J. For. Res. 33, 385–397.
Landsberg, J., 2003b. Physiology in forest models: history and the future. For. Biomet. Model. Inform. Sci. 1, 49–63.
Landsberg, J.J., Ludlow, M.M., 1970. A technique for determining resistance to mass transfer through the boundary layers of plants with complex structure. J. Appl. Ecol. 7, 187–192.
Landsberg, J.J., Waring, R.H., 1997. A generalised model of forest productivity using simplified concepts of radiation-use efficiency, carbon balance and partitioning. For. Ecol. Manag. 95, 209–228.
Laprise, R., Caya, D., Frigon, A., Paquin, D., 2003. Current and perturbed climate as simulated by the second-generation Canadian Regional Climate Model (CRCM-II) over northwestern North America. Clim. Dyn. 21, 405–421.
Laroque, C.P., Smith, D.J., 2003. Radial-growth forecasts for five high-elevation conifer species on Vancouver Island, British Columbia. For. Ecol. Manag. 183, 313–325.
Leuning, R., 1995. A critical appraisal of a combined stomatal-photosynthesis model for C_3 plants. Plant Cell Environ. 18, 339–355.
Linkosalo, T., 2000. Mutual regularity of spring phenology of some boreal tree species: predicting with other species and phenological models. Can. J. For. Res. 30, 667–673.
Loehle, C., LeBlanc, D., 1996. Model-based assessments of climate change effects on forests: a critical review. Ecol. Model. 90, 1–31.
Mäkinen, H., Nöjd, P., Saranpää, P., 2003. Seasonal changes in stem radius and production of new tracheids in Norway spruce. Tree Physiol. 23, 959–968.
Malhi, Y., Baldocchi, D.D., Jarvis, P.G., 1999. The carbon balance of tropical, temperate and boreal forests. Plant Cell Environ. 22, 715–740.
Manitoba Provincial Parks Branch, 1973. Outdoor Recreation Master Plan: Duck Mountain Provincial Park. Manitoba Department of Tourism, Recreation and Cultural Affairs, Winnipeg, Manitoba.
Mekis, E., Hogg, W.D., 1999. Rehabilitation and analysis of Canadian daily precipitation time series. Atmosphere-Ocean 37, 53–85.
Middleton, E.M., Sullivan, J.H., Bovard, B.D., Deluca, A.J., Chan, S.S., Cannon, T.A., 1997. Seasonal variability in foliar characteristics and physiology for boreal forest species at the five Saskatchewan tower sites during the 1994 Boreal Ecosystem-Atmosphere Study. J. Geophys. Res. 102 (24), 28831–28844.
Misson, L., 2004. MAIDEN: a model for analyzing ecosystem processes in dendroecology. Can. J. For. Res. 34, 874–887.
Misson, L., Rathgeber, C., Guiot, J., 2004. Dendroecological analysis of climatic effects on *Quercus petraea* and *Pinus halepensis* radial growth using the process-based MAIDEN model. Can. J. For. Res. 34, 888–898.
Morris, D.M., Gordon, A.G., Gordon, A.M., 2003. Patterns of canopy interception and throughfall along a topographic sequence for black spruce dominated forest ecosystems in northwestern Ontario. Can. J. For. Res. 33, 1046–1060.
Mudelsee, M., 2003. Estimating Pearson's correlation coefficient with bootstrap confidence interval from serially dependent time series. Math. Geol. 35, 651–665.
Myking, T., Heide, O.M., 1995. Dormancy release and chilling requirement of buds of latitudinal ecotypes of *Betula pendula* and *B. pubescens*. Tree Physiol. 15, 697–704.
Nakicenovic, N., Alcamo, J., Davis, G., et al., 2000. IPCC Special Report on Emissions Scenarios. Cambridge University Press, Cambridge, 599 pp.
Newcomer, J., Landis, D., Conrad, S., Curd, S., Huemmrich, K., Knapp, D., Morrell, A., Nickeson, J., Papagno, A., Rinker, D., Strub, R., Twine, T., Hall, F., Sellers, P., 2000. Collected Data of the Boreal Ecosystem-Atmosphere Study. CD-ROM. NASA, Goddard Space Flight Center, Greenbelt, MD.
Peng, C., Apps, M.J., 1999. Modelling the response of net primary productivity (NPP) of boreal forest ecosystems to changes in climate and fire disturbance regimes. Ecol. Model. 122, 175–193.
Perala, D.A., 1990. *Populus tremuloides* Michx. In: Burns, R.M., Honkala, B.H. (Eds.), Silvics of North America, vol. 2. Hardwoods. U.S.D.A. Forest Service Agriculture Handbook 654, Washington, DC.
Rathgeber, C., Nicault, A., Guiot, J., Keller, T., Guibal, F., Roche, P., 2000. Simulated responses of *Pinus halepensis* forest

productivity to climatic change and CO_2 increase using a statistical model. Global Planet. Change 26, 405–421.
Rathgeber, C., Nicault, A., Kaplan, J.O., Guiot, J., 2003. Using a biogeochemistry model in simulating forests productivity responses to climatic change and [CO_2] increase: example of *Pinus halepensis* in Provence (south-east France). Ecol. Model. 166, 239–255.
Rathgeber, C.B.K., Misson, L., Nicault, A., Guiot, J., 2005. Bioclimatic model of tree radial growth: application to the French Mediterranean Aleppo pine forests. Trees-Struct. Funct. 19, 162–176.
Raulier, F., Bernier, P.Y., Ung, C.H., 2000. Modeling the influence of temperature on monthly gross primary productivity of sugar maple stands. Tree Physiol. 20, 333–345.
Raulier, F., Bernier, P.Y., Ung, C.-H., Boutin, R., 2002. Structural differences and functional similarities between two sugar maple (*Acer saccharum*) stands. Tree Physiol. 22, 1147–1156.
Robinson, A.P., Ek, A.R., 2000. The consequences of hierarchy for modeling in forest ecosystems. Can. J. For. Res. 30, 1837–1846.
Roeckner, E., Arpe, K., Bengtsson, L., Christoph, M., Claussen, M., Dümenil, L., Esch, M., Giorgetta, M., Schlese, U., Schulzweida, U., 1996. The Atmospheric General Circulation Model ECHAM-4: Model Description and Simulation of Present-day Climate. Report No. 218, the Max Planck Institute for Meteorology, Hamburg, Germany, 90 pp.
Rossi, S., Deslauriers, A., Anfodillo, T., Morin, H., Saracino, A., Motta, R., Borghetti, M., 2006. Conifers in cold environments synchronize maximum growth rate of tree-ring formation with day length. New Phytol. 170, 301–310.
Rudolph, T.D., Laidly, P.R., 1990. *Pinus banksiana* Lamb. In: Burns, R.M., Honkala, B.H. (Eds.), Silvics of North America, vol. 1. Conifers. U.S.D.A. Forest Service Agriculture Handbook 654, Washington, DC.
Sellers, P.J., Hall, F.G., Kelly, R.D., Black, T.A., Baldocchi, D., Berry, J., Ryan, M., Jon Ranson, K., Crill, P.M., Lettenmaier, D.P., Margolis, H., Cihlar, J., Newcomer, J., Fitzjarrald, D., Jarvis, P.G., Gower, S.T., Halliwell, D., Williams, D., Goodison, B., Wickland, D.E., Guertin, F.E., 1997. BOREAS in 1997: experiment overview, scientific results and future directions. J. Geophys. Res. 102 (D24), 28731–28769.
Smith, W.K., 1980. Importance of aerodynamic resistance to water use efficiency in three conifers under field conditions. Plant Physiol. 65, 132–135.
Snowdon, P., 2001. Short-term predictions of growth of *Pinus radiata* with models incorporating indices of annual climatic variation. For. Ecol. Manag. 152, 1–11.
Spittlehouse, D.L., Stewart, R.B., 2003. Adaptation to climate change in forest management. BC J. Ecosyst. Manag. 4, 1–11.
Sutton, A., Tardif, J., 2005. Distribution and anatomical characteristics of white rings in *Populus tremuloides*. IAWA J. 26, 221–238.
Sutton, A., Tardif, J.C., 2007. Dendrochronological reconstruction of forest tent caterpillar outbreaks in time and space, western Manitoba, Canada. Can. J. For. Res. 37, 1643–1657.
Systat Software Inc., 2004. SYSTAT Version 11.0 Software. SPSS Inc., Chicago, IL, USA.
Tardif, J., 2004. Fire history in the Duck Mountain Provincial Forest, Western Manitoba Sustainable Forest Management Network. Project Reports 2003/2004 Series. University of Alberta, Edmonton, Alberta, 30 pp.
Tardif, J., Bergeron, Y., 1997. Comparative dendroclimatological analysis of two black ash and two white cedar populations from contrasting sites in the Lake Duparquet region, northwestern Québec. Can. J. For. Res. 27, 108–116.
Tardif, J., Conciatori, F., Bergeron, Y., 2001a. Comparative analysis of the climatic response of seven boreal tree species from northwestern Québec, Canada. Tree-Ring Res. 57, 169–181.
Tardif, J., Flannigan, M., Bergeron, Y., 2001b. An analysis of the daily radial activity of 7 boreal tree species, northwestern Quebec. Environ. Monit. Assess. 67, 141–160.
Tardif, J.C., Conciatori, F., 2006. Influence of climate on tree rings and vessel features in red oak and white oak growing near their northern distribution limit, southwestern Quebec, Canada. Can. J. For. Res. 36, 2317–2330.
Van Wagner, C.E., 1987. Development and structure of the Canadian Forest Fire Weather Index System. Forestry Technical Report 35. Canadian Forest Service, Ottawa, Ontario, 37 pp.
Viereck, L.A., Johnston, W.F., 1990. *Picea mariana* (Mill.) B.S.P. In: Burns, R.M., Honkala, B.H. (Eds.), Silvics of North America, vol. 1. Conifers. U.S.D.A. Forest Service Agriculture Handbook 654, Washington, DC.
Vincent, L.A., Gullett, D.W., 1999. Canadian historical and homogeneous temperature datasets for climate change analyses. Int. J. Climatol. 19, 1375–1388.
Waring, R.H., Landsberg, J.J., Williams, M., 1998. Net primary production of forests: a constant fraction of gross primary production? Tree Physiol. 18, 129–134.
Weber, M.G., Flannigan, M.D., 1997. Canadian boreal forest ecosystem structure and function in a changing climate: impact on fire regimes. Environ. Rev. 5, 145–166.
Woodhouse, C.A., 1999. Artificial neural networks and dendroclimatic reconstructions: an example from the Front Range, Colorado, USA. Holocene 9, 521–529.
Woodward, F.I., Osborne, C.P., 2000. The representation of root processes in models addressing the responses of vegetation to global change. New Phytol. 147, 223–232.
Woollons, R.C., Snowdon, P., Mitchell, N.D., 1997. Augmenting empirical stand projection equations with edaphic and climatic variables. For. Ecol. Manag. 98, 267–275.
Zahner, R., 1968. Water deficits and growth of trees. In: Kozlowski, T.T. (Ed.), Water Deficits and Plant Growth, vol. II. Academic Press, New York, NY, USA, pp. 191–254.
Zar, J.H., 1999. Biostatistical Analysis, 4th ed. Prentice Hall, NJ, 663 pp.